H. B. Simmons
Seabrook

TIDAL FLOW IN ENTRANCES

by

JOHN L. FRENCH

TECHNICAL BULLETIN NO. 3

January 1960

Committee on Tidal Hydraulics
CORPS OF ENGINEERS, U. S. ARMY

Report Documentation Page

Form Approved
OMB No. 0704-0188

1. REPORT DATE	2. REPORT TYPE	3. DATES COVERED
01 JAN 1960	**N/A**	**-**

4. TITLE AND SUBTITLE	5a. CONTRACT NUMBER
Tidal Flow in Entrances	5b. GRANT NUMBER
	5c. PROGRAM ELEMENT NUMBER
6. AUTHOR(S)	5d. PROJECT NUMBER
French, J. L.	5e. TASK NUMBER
	5f. WORK UNIT NUMBER
7. PERFORMING ORGANIZATION NAME(S) AND ADDRESS(ES)	8. PERFORMING ORGANIZATION REPORT NUMBER
U.S. Army, Committee on Tidal Hydraulics	**Technical Bulletin No. 3**
9. SPONSORING/MONITORING AGENCY NAME(S) AND ADDRESS(ES)	10. SPONSOR/MONITOR'S ACRONYM(S)
	11. SPONSOR/MONITOR'S REPORT NUMBER(S)

12. DISTRIBUTION/AVAILABILITY STATEMENT
Approved for public release, distribution unlimited

13. SUPPLEMENTARY NOTES

14. ABSTRACT

15. SUBJECT TERMS

16. SECURITY CLASSIFICATION OF:			17. LIMITATION OF ABSTRACT	18. NUMBER OF PAGES	19a. NAME OF RESPONSIBLE PERSON
a. REPORT	b. ABSTRACT	c. THIS PAGE			
unclassified	**unclassified**	**unclassified**	**UU**	**73**	

Standard Form 298 (Rev. 8-98)
Prescribed by ANSI Std Z39-18

REPORTS OF COMMITTEE ON TIDAL HYDRAULICS

Report No.	Title	Date
1	Evaluation of Present State of Knowledge of Factors Affecting Tidal Hydraulics and Related Phenomena	Feb. 1950
2	Bibliography on Tidal Hydraulics	Feb. 1954
	Supplement No. 1, Material Compiled Through May 1955	June 1955
	Supplement No. 2, Material Compiled from May 1955 to May 1957	May 1957
	Supplement No. 3, Material Compiled from May 1957 to May 1959	May 1959

Technical Bulletin No.	Title	Date
1	Sediment Discharge Measurements in Tidal Waterways	May 1954
2	Fresh Water-Salt Water Density Currents, A Major Cause of Siltation in Estuaries	April 1957

U. S. Army, Committee on Tidal Hydraulics, CE, TIDAL FLOW IN ENTRANCES, by J. L. French. January 1960, 54 pp - tables. (Technical Bulletin No. 3)

Unclassified report

This report comprises two analytical studies. In the first, the methods of potential theory are applied to the problem of determining the velocities in the approaches to a canal connecting an ocean with a lagoon or bay. Entrances with and without jetties extending into the ocean are considered. The streamlines are determined and velocities along the streamlines are given in a form suitable for simple application to engineering problems. In the second study, Tollmien's analyses for (1) the free jet boundary and (2) jet efflux from a linear slot are applied to the problem of the efflux of a two-dimensional jet from a slot of definite width with particular reference to jet flow from a channel into a region of surrounding quiet water, such as an ocean. The literature was searched for appropriate experimental data, and the constant of Tollmien's theory is evaluated accordingly. The streamlines are determined, and velocities along the streamlines computed and presented in a manner susceptible of simple application to practical engineering problems.

UNCLASSIFIED

1. Estuaries
2. Flow of water--Open channels
3. Jets
4. Tidal inlets

I. French, J. L.
II. Committee on Tidal Hydraulics, Technical Bulletin No. 3

U. S. Army, Committee on Tidal Hydraulics, CE, TIDAL FLOW IN ENTRANCES, by J. L. French. January 1960, 54 pp - tables. (Technical Bulletin No. 3)

Unclassified report

This report comprises two analytical studies. In the first, the methods of potential theory are applied to the problem of determining the velocities in the approaches to a canal connecting an ocean with a lagoon or bay. Entrances with and without jetties extending into the ocean are considered. The streamlines are determined and velocities along the streamlines are given in a form suitable for simple application to engineering problems. In the second study, Tollmien's analyses for (1) the free jet boundary and (2) jet efflux from a linear slot are applied to the problem of the efflux of a two-dimensional jet from a slot of definite width with particular reference to jet flow from a channel into a region of surrounding quiet water, such as an ocean. The literature was searched for appropriate experimental data, and the constant of Tollmien's theory is evaluated accordingly. The streamlines are determined, and velocities along the streamlines computed and presented in a manner susceptible of simple application to practical engineering problems.

UNCLASSIFIED

1. Estuaries
2. Flow of water--Open channels
3. Jets
4. Tidal inlets

I. French, J. L.
II. Committee on Tidal Hydraulics, Technical Bulletin No. 3

U. S. Army, Committee on Tidal Hydraulics, CE, TIDAL FLOW IN ENTRANCES, by J. L. French. January 1960, 54 pp - tables. (Technical Bulletin No. 3)

Unclassified report

This report comprises two analytical studies. In the first, the methods of potential theory are applied to the problem of determining the velocities in the approaches to a canal connecting an ocean with a lagoon or bay. Entrances with and without jetties extending into the ocean are considered. The streamlines are determined and velocities along the streamlines are given in a form suitable for simple application to engineering problems. In the second study, Tollmien's analyses for (1) the free jet boundary and (2) jet efflux from a linear slot are applied to the problem of the efflux of a two-dimensional jet from a slot of definite width with particular reference to jet flow from a channel into a region of surrounding quiet water, such as an ocean. The literature was searched for appropriate experimental data, and the constant of Tollmien's theory is evaluated accordingly. The streamlines are determined, and velocities along the streamlines computed and presented in a manner susceptible of simple application to practical engineering problems.

UNCLASSIFIED

1. Estuaries
2. Flow of water--Open channels
3. Jets
4. Tidal inlets

I. French, J. L.
II. Committee on Tidal Hydraulics, Technical Bulletin No. 3

U. S. Army, Committee on Tidal Hydraulics, CE, TIDAL FLOW IN ENTRANCES, by J. L. French. January 1960, 54 pp - tables. (Technical Bulletin No. 3)

Unclassified report

This report comprises two analytical studies. In the first, the methods of potential theory are applied to the problem of determining the velocities in the approaches to a canal connecting an ocean with a lagoon or bay. Entrances with and without jetties extending into the ocean are considered. The streamlines are determined and velocities along the streamlines are given in a form suitable for simple application to engineering problems. In the second study, Tollmien's analyses for (1) the free jet boundary and (2) jet efflux from a linear slot are applied to the problem of the efflux of a two-dimensional jet from a slot of definite width with particular reference to jet flow from a channel into a region of surrounding quiet water, such as an ocean. The literature was searched for appropriate experimental data, and the constant of Tollmien's theory is evaluated accordingly. The streamlines are determined, and velocities along the streamlines computed and presented in a manner susceptible of simple application to practical engineering problems.

UNCLASSIFIED

1. Estuaries
2. Flow of water--Open channels
3. Jets
4. Tidal inlets

I. French, J. L.
II. Committee on Tidal Hydraulics, Technical Bulletin No. 3

TIDAL FLOW IN ENTRANCES

by

JOHN L. FRENCH

TECHNICAL BULLETIN NO. 3

January 1960

Committee on Tidal Hydraulics
CORPS OF ENGINEERS, U. S. ARMY

ARMY-MRC VICKSBURG, MISS.

PREFACE

The Corps of Engineers, Department of the Army, is charged by Congress with the responsibility of establishing and maintaining navigable channels to the major seaports of the United States. This responsibility frequently involves the establishment of a navigable channel at tidal inlets and estuaries. To advise the Chief of Engineers in this phase of his work, a Committee on Tidal Hydraulics has been set up within the Corps of Engineers. This Committee, among other duties, arranges to have technical studies made of various problems connected with the establishment and maintenance of channels in tidal waterways.

One of the problems encountered at tidal entrances is that of flow patterns - velocity and direction - which develop at the various inlets selected for navigation improvements. This problem has not received sufficient attention in the past to bring about a quantitative understanding of these flow patterns. As one step in overcoming this lack of understanding, the Committee requested assistance from the Mechanics Division of the Bureau of Standards in laying the theoretical groundwork for the solution of this problem. Arrangements for this assistance were made by the Beach Erosion Board of the Corps of Engineers in a letter, dated 20 October 1950, to the National Bureau of Standards.

The problem, in effect, has two, more or less independent aspects: the definition of the pattern of flow from the ocean into the inlet, and the definition of the pattern of flow from the inlet into the ocean. These two aspects can be conveniently handled separately, and the National Bureau of Standards reported on them separately to the Committee in 1951. The committee has chosen to publish the two reports together in this volume, but

has maintained the separation of the two studies in the publication.

The funds available did not permit as extensive an exploration of these problems as is desirable. However, the two reports that have been prepared are believed to represent a valuable contribution to the literature on this subject. Certain simplifying assumptions were made in both cases, and only a limited number of conditions were investigated; these are explained in detail in the report.

Velocity Pattern at Entrance

The first part of the report, prepared by John L. French, National Bureau of Standards, deals with the pattern developed by flow from the ocean into an inlet. For this study, the following simplifying assumptions were made:

a. The depth was uniform and the same in the ocean and the inlet.

b. The effect of viscosity was neglected.

Two forms of inlets were considered: an inlet without jetties, and an inlet with jetties extending into the ocean.

The author recognized that the simplifications introduced into the analysis would prevent an exact correlation between the flow patterns developed by his study and actual flow patterns under field conditions. He points out that this discrepancy would become more and more evident at points downstream from the entrance where diffusion would cause the jet to spread over the entire width of the jetty channel.

This analysis can be used to predict the flow direction and velocity pattern at the inlet for conditions of uniform depth and unobstructed approaches. The presence of shoals or other obstacles would, of course, cause the actual flow pattern to vary from the predicted patterns of streamlines as shown in figs. 5 and 8 of the report. An example of the use of this analysis of flow at tidal entrances is given in Appendix A to this report.

Flow Pattern at Exit

The second part of the report, also prepared by Mr. French, deals with the pattern of flow from an inlet into the ocean. The physical aspects of this problem suggest similarity to the diffusion of a submerged two-dimensional jet, and the velocity profiles have been developed on this basis. An example of the use of this analysis of discharge from an inlet into the ocean is given in Appendix B.

ACKNOWLEDGMENT

The author is indebted to Dr. Garbis H. Keulegan of the National Bureau of Standards' staff for the formulation of the two problems herein discussed and for many valuable suggestions during the conduct of the investigation.

CONTENTS

	Page
PREFACE	iii
ACKNOWLEDGMENT	vii
PART I: THE VELOCITY DISTRIBUTION AT THE ENTRANCE	1
Scope of Investigation	1
The Present Problem	1
Previous Treatment of Free Streamline Flow	3
Determination of Velocity Distribution	5
Status of Problem	23
References	24
PART II: THE VELOCITY DISTRIBUTION IN THE JET ISSUING FROM A CHANNEL INTO AN OCEAN OR LAGOON	25
Introduction	25
Statement of Problem	26
General Considerations	28
Application of Theory	32
Summary	47
Status of Problem	47
References	49
TABLES 1-5	
APPENDIX A: APPLICATION OF A CONTRACTING FLOW NET TO A SPECIFIC CONDITION	A1
TABLE A1	
APPENDIX B: APPLICATION OF AN EXPANDING FLOW NET TO A SPECIFIC CONDITION	B1
TABLE B1	

TIDAL FLOW IN ENTRANCES

PART I: THE VELOCITY DISTRIBUTION AT THE ENTRANCE

Scope of Investigation

1. At a conference between Dr. Martin A. Mason of the Beach Erosion Board and Dr. Garbis H. Keulegan of the National Bureau of Standards, the scope of the project was defined in detail and the following four aspects of tidal flow from an ocean through a relatively short channel into a lagoon were agreed upon for the investigation:

a. Velocity distribution at the entrance.

b. Velocity distribution at the exit.

c. Determination of the mean velocity in the channel.

d. Velocity distribution in the channel.

The Present Problem

2. Part I of this report is confined to the first problem listed above--the velocity distribution of the water as it approaches and enters the connecting channel between the ocean and the lagoon.

3. Fig. 1 is a definition sketch of the ocean, connecting channel, and lagoon. Inasmuch as the ocean, connecting channel, and lagoon in question are assumed to be subject to tidal action, this aspect of the investigation will apply to flow from the lagoon to the ocean as well as flow from the ocean to the lagoon. The various factors affecting the velocity distribution at and near the entrance include, in addition to the shape or geometry of the entrance itself, the variation in depth of the ocean or

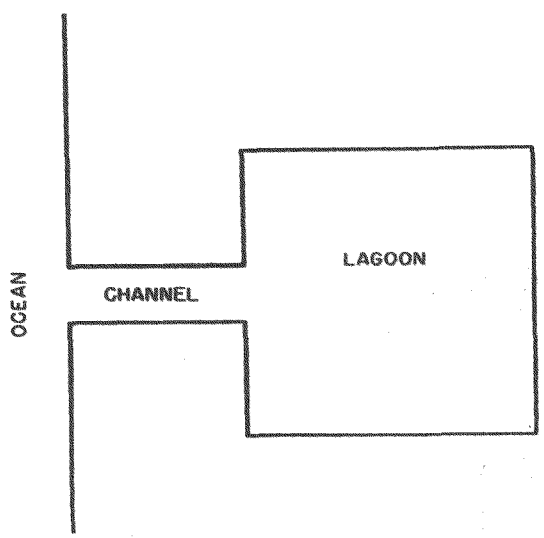

Fig. 1. Definition sketch of problem

lagoon as the entrance is approached, the presence of littoral currents, the effect of frictional resistance on the flow, the effect of wave action, and if fresh-water drainage occurs in the lagoon, the effect of density currents. The effects of littoral currents, wave action, and possible density currents on the velocity distribution were not originally contemplated as forming a part of the project. For the present, the effect of frictional resistance and the effect of changing depth in the ocean or lagoon as the channel entrance is approached will be neglected. Hence the present problem resolves itself into the effect of various channel-entrance shapes on the velocity distribution of a two-dimensional flow of a perfect fluid from a large body of water into a relatively narrow channel entrance.

4. The velocity picture at the entrance will be determined by the methods applicable to free streamlines, methods devised by Helmholtz and Kirchhoff and later elaborated by various investigators. If fluid particles in flowing around a sharp corner of radius zero are assumed to remain in contact with the bounding surface, an infinite acceleration of the fluid particles is required to accomplish this result. This in turn requires that the velocity and pressure be infinite at the corner. In order to overcome this difficulty, Helmholtz introduced the concept of free streamlines, in which the assumption is made that separation occurs in the flow of fluid particles around sharp corners. Thus, downstream from abrupt changes in the bounding surface, such as those considered in this report, the streamlines of the flow are separated from the boundary by an area occupied by fluid assumed to be at rest.

5. With real fluids, owing to viscosity, the motion is so modified, of course, that points of infinite velocity and pressure do not occur, nor does the fluid between the free streamline and the bounding surface remain at rest; it is in eddying motion. With the assumption of free streamlines, the velocity and hence the pressure at abrupt corners is finite, and to this extent the solutions by this method of various flow problems involving flow around sharp corners are more physically acceptable than solutions by methods that indicate infinite velocities at such points. Nevertheless, owing to the fact that with real fluids the region of fluid assumed to be at rest in the theory is actually in motion through the effect of viscosity, solutions by means of free streamlines must be regarded as approximations

which become less and less valid as one proceeds downstream from the point of separation. The region between the free streamline and the channel wall is in eddying motion, and the lateral diffusion of the eddies as they move downstream obliterates the potential core of the jet and causes the outside jet boundaries to expand to the full width of the channel at a distance on the order of 10 channel widths from the entrance.

6. Under these circumstances, the use of the free streamline method to determine velocity distributions at distances in excess of approximately two or three channel widths downstream from the entrance would not be warranted.

7. The solutions in this report are given in graphical form, i.e., the streamlines are shown and the velocities along the streamlines are given in terms of the free streamline velocity and also in terms of the mean velocity in the channel. The mean velocity in the channel must be determined from a consideration of the tidal fluctuations in the ocean and lagoon, and the dimensions and roughness of the connecting channel. This problem will be considered in a later report on this project.

Previous Treatment of Free Streamline Flow

8. The literature is replete with investigations of two-dimensional flow problems in which the bounding surfaces take the form of possible channel-entrance shapes. Unfortunately, however, these problems have been almost exclusively considered from the standpoint of determining the equations of the free streamlines and the coefficient of contraction. The computation of the equipotential lines and streamlines in the body of the flowing fluid has been, in the great majority of cases, entirely omitted.

9. The literature on two-dimensional fluid flow problems that might have application to certain tidal-entrance shapes is so extensive that all the references cannot be individually described herein. Indeed, the investigations have been so numerous that although an extensive search of the literature was made, it was by no means exhaustive, and could not have been in view of the time limitation on the project. Nevertheless, a short résumé of the more important references is believed warranted.

10. First, most of the standard references in hydrodynamics such as

Lamb[4*] and Milne-Thompson[6] treat the free streamline, two-dimensional flow through an aperture in a plane wall, and through a channel corresponding to the two-dimensional form of Borda's mouthpiece. Without exception, the treatment is from the viewpoint of determining the equation of the free streamline and determining the coefficient of contraction of the jet.

11. Prasil[7] gives a solution of the two-dimensional, free streamline flow through an aperture in a plane wall and shows a flow net. However, the scale of the coordinate system is not given, and other inadequacies limit the usefulness of the flow net given.

12. Greenhill[2] has solved a variety of problems in two-dimensional flow which have application to possible channel entrances of various shapes. Among these are those shown in fig. 2. The angle ϕ in fig. 2(a) and 2(b) may be varied to give solutions to many special problems, among them being most of those treated by von Mises.[9]

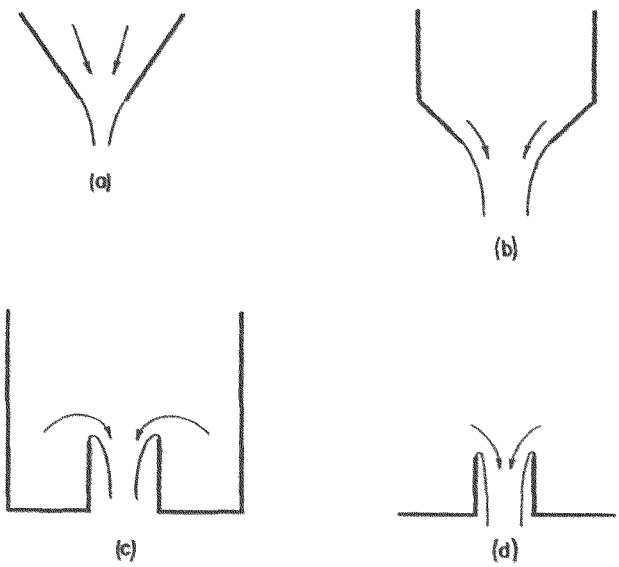

Fig. 2. Two-dimensional flow boundaries

13. Michell[5] also, among many others, solved the problem of the modified Borda's mouthpiece shown in fig. 2(d).

14. Greenhill,[3] using primarily the work of Cisotti, Levi-Civita, Levy, and others, has given solutions to many two-dimensional flow patterns involving curved boundaries. Some of these are shown in fig. 3.

15. Cisotti[1] has also published solutions to most of the flow problems shown in figs. 2 and 3.

16. The references cited above give solutions to the various problems indicated, generally by giving the functional relation between the complex potential and a parameter, which in turn is related through

---

* Raised numbers refer to references at the end of this part (Part I).

another functional expression to the physical z plane. The actual determination of the equipotential and streamlines necessary for the present problem was not done.

17. In general, the work involved in applying the foregoing solutions to the determination of the flow net is not difficult; nevertheless, it is in most cases tedious, and the amount of labor involved is by no means small. For this reason, it has been impossible with the time at our disposal to utilize all the material available and to compute the flow net for all the boundary forms shown in figs. 2 and 3. In the remainder of this report, the equipotential and streamlines for the two-dimensional flow through an aperture in a plane wall and through the two-dimensional form of a Borda's mouthpiece have been determined. Inasmuch as any streamline may be replaced by a bounding surface without in any way disturbing the flow pattern, these two examples will yield a fairly representative group of possible channel entrances. It is nevertheless regretted that more of the examples cited could not have been applied to the present problem, and it is believed that the future application of these two-dimensional flow solutions to the determination of the equipotential and streamlines for the various shapes of possible channel entrances will prove a useful tool in the practical solution of the tidal-entrance problem.

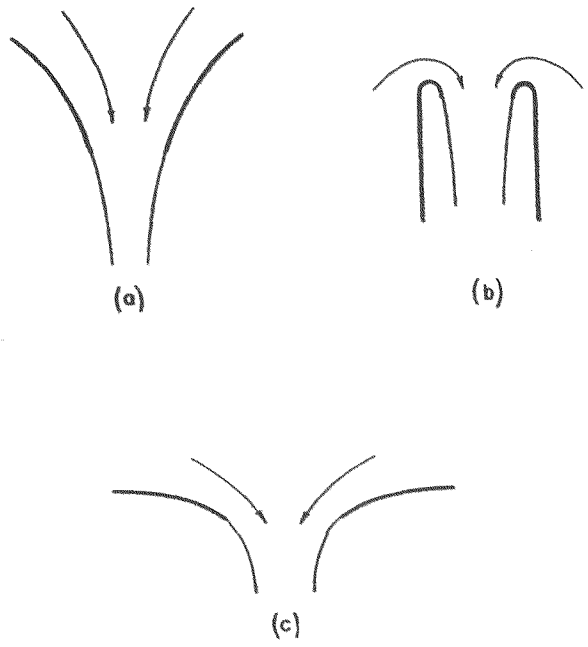

Fig. 3. Two-dimensional flow with curved boundaries

Determination of Velocity Distribution

Preliminary considerations

18. In the problem we are considering herein, the flow into the relatively short channel from the ocean or from the lagoon will vary, of

course, with the difference in surface elevation between the two bodies of water. Since this difference in elevation is caused by tidal action, the flow into the channel will vary with time. However, since the tidal action will vary slowly with time, we can for all practical purposes consider the problem of the velocity distribution at the channel entrance as being one involving steady flow only.

19. Owing to the fact that the velocity along a streamline will vary as the channel entrance is approached, it is obvious from a consideration of Bernoulli's equation that the surface elevation will vary. However, the velocities that are encountered in tidal channels are such that the variation in surface elevation due to variation in velocities will be small compared to the depth of the channel. Therefore, insofar as surface variations are concerned, the problem may be considered for practical purposes to be essentially two-dimensional. As noted previously, the effects of friction and variation in depth of the ocean as the channel entrance is approached will be treated in a subsequent report, and for the present, constant depth and nonviscous flow are assumed.

20. Under these conditions, the methods of conformal mapping have direct application to the problem of obtaining the velocity distribution at the channel entrance. For irrotational, two-dimensional, steady-flow problems it is necessary only that Laplace's equation in two dimensions be satisfied, and that the boundary conditions regarding coincidence of streamlines with fixed boundaries be observed. Where there is a free streamline, the further requirement is made that the pressure and hence the velocity along the free streamline be constant.

21. The ability of the processes of conformal transformations to satisfy the above-mentioned requirements and hence to provide solutions to irrotational, two-dimensional flow problems has been amply demonstrated in most of the standard references on hydrodynamics, and there is no need to repeat the argument herein.

Entrance analogous to
two-dimensional orifice

22. This is the type of entrance from the ocean to the channel (and from the lagoon to the channel) shown in fig. 1.

23. Proceeding by the usual methods of conformal mapping,

Greenhill (page 33 of reference 2) has shown for the flow orientation given in fig. 4 that the relation between the flow pattern in the physical plane $z = x + i\,y$ of the flow, and the complex potential $W = \phi + i\psi$, where ϕ and ψ are respectively the potential and stream functions, is given by

$$1/2\,\frac{\pi z}{c} = \log\frac{\zeta + 1}{\zeta - 1} - \zeta \qquad (1)$$

and

$$\sinh\,\Omega = e\,\frac{\pi W}{Q} \qquad (2)$$

where ζ is related to W, Ω, and other characteristics of the flow through the relation

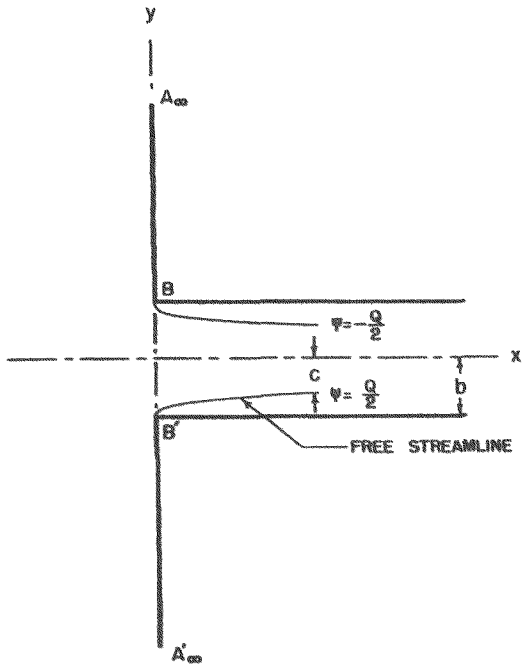

Fig. 4. Channel entrance corresponding to a two-dimensional orifice

$$\zeta = -V\,\frac{dz}{dW} = \frac{V}{q}\,e^{i\theta} = e^{\Omega} \qquad (3)$$

In the preceding expressions, c is the half-width of the jet at infinity as shown in fig. 4; V is the velocity along the free streamline and also the velocity of the jet at infinity; θ is the angle that the velocity vector makes with the positive x-axis; Q is the rate of discharge per unit depth of channel and therefore has the dimensions of a velocity multiplied by a length; and q is the velocity at any point x, y in the flow pattern. The potential and stream functions ϕ and ψ are related to the x and y velocity components through the expressions

$$\frac{\partial\phi}{\partial x} = -u = \frac{\partial\psi}{\partial y}$$

and

$$\frac{\partial\phi}{\partial v} = -v = \frac{\partial\psi}{\partial v}$$

where u is the component of the velocity vector in the x direction and v is the y component. Obviously ϕ and ψ have the dimensions of a velocity multiplied by a length so that $\pi W/Q$ and consequently ζ and Ω are dimensionless.

24. Equation 1 has been derived on the basis that the zero potential line passes through the two points B and B'.

25. In equation 2, replacing Ω by its value $\Omega = \log \zeta$ from equation 3, and replacing the hyperbolic sine by its exponential form, we have

$$1/2 \left[\zeta - \frac{1}{\zeta}\right] = e^{\frac{\pi W}{Q}}$$

which yields

$$\zeta = e^{\frac{\pi W}{Q}} \pm \sqrt{e^{\frac{2\pi W}{Q}} + 1} \qquad (4)$$

and since ζ is infinite when W is infinite, we must use the positive sign and

$$\zeta = e^{\frac{\pi W}{Q}} + \sqrt{e^{\frac{2\pi W}{Q}} + 1} \qquad (5)$$

Or we may write

$$\zeta = e^{\frac{\pi W}{Q}} \left[1 + \sqrt{1 + e^{-\frac{2\pi W}{Q}}}\right] \qquad (6)$$

26. The real and imaginary parts of ζ may be conveniently determined by replacing the terms under the radicals in equations 5 and 6 by their equivalent series forms. The binomial expansion equivalent to the radical term in equation 5 will be convergent for negative values of the potential ϕ, and equation 6 may be used to compute ζ for positive values of ϕ. Therefore, letting ξ and η be the real and imaginary parts of ζ, determined from equations 5 and 6, we have

$$\zeta = \xi + i\,\eta \qquad (7)$$

27. Substituting this expression for ζ into equation 1, and separating the reals and imaginaries

$$1/2\,\frac{\pi x}{c} + \xi = \log \frac{\left[(\xi + 1)^2 + \eta^2\right]^{1/2}}{\left[(\xi - 1)^2 + \eta^2\right]^{1/2}} \tag{8}$$

and

$$1/2\,\frac{\pi y}{c} + \eta = \tan^{-1}\frac{\eta}{\xi + 1} - \tan^{-1}\frac{\eta}{\xi - 1} \tag{9}$$

28. Letting b be the half-width of the channel as indicated in fig. 4, we have $y = -b$ at $\phi = 0$ and $\psi = Q/2$, from which by equation 4, $\zeta = i$ at the point B'. Substitution in equation 9 gives

$$\frac{c}{b} = \frac{\pi}{2 + \pi} \tag{10}$$

and equations 8 and 9 become

$$\frac{2 + \pi}{2}\,\frac{x}{b} + \xi = \log \frac{\left[(\xi + 1)^2 + \eta^2\right]^{1/2}}{\left[(\xi - 1)^2 + \eta^2\right]^{1/2}} \tag{11}$$

$$\frac{2 + \pi}{2}\,\frac{y}{b} + \eta = \tan^{-1}\frac{\eta}{\xi + 1} - \tan^{-1}\frac{\eta}{\xi - 1} \tag{12}$$

29. Equations 7, 11, and 12 permit the computation of the coordinates in the z plane corresponding to any value of the complex potential W. These equations have been used to compute values of x/b and y/b corresponding to various values of $\pi\phi/Q$ and ψ/Q. The results are given in table 1. In fig. 5 the data of table 1 have been used to plot the streamlines and equipotential lines of the flow net. Comparison of fig. 5 with fig. 4 will show that the orientation differs by 180°. This was done merely for convenience in drawing fig. 5.

30. Since the velocity is tangential to the streamlines at all points, the data of fig. 5 indicate the direction of the current as it approaches the channel entrance. The problem of determining the magnitude of the velocity remains.

31. Since $q = \partial\phi/\partial s$, where q is the velocity measured in the direction of s, the velocity could be approximated from fig. 5 by determining the potential gradient $\partial\phi/\partial s$ along the streamlines. However,

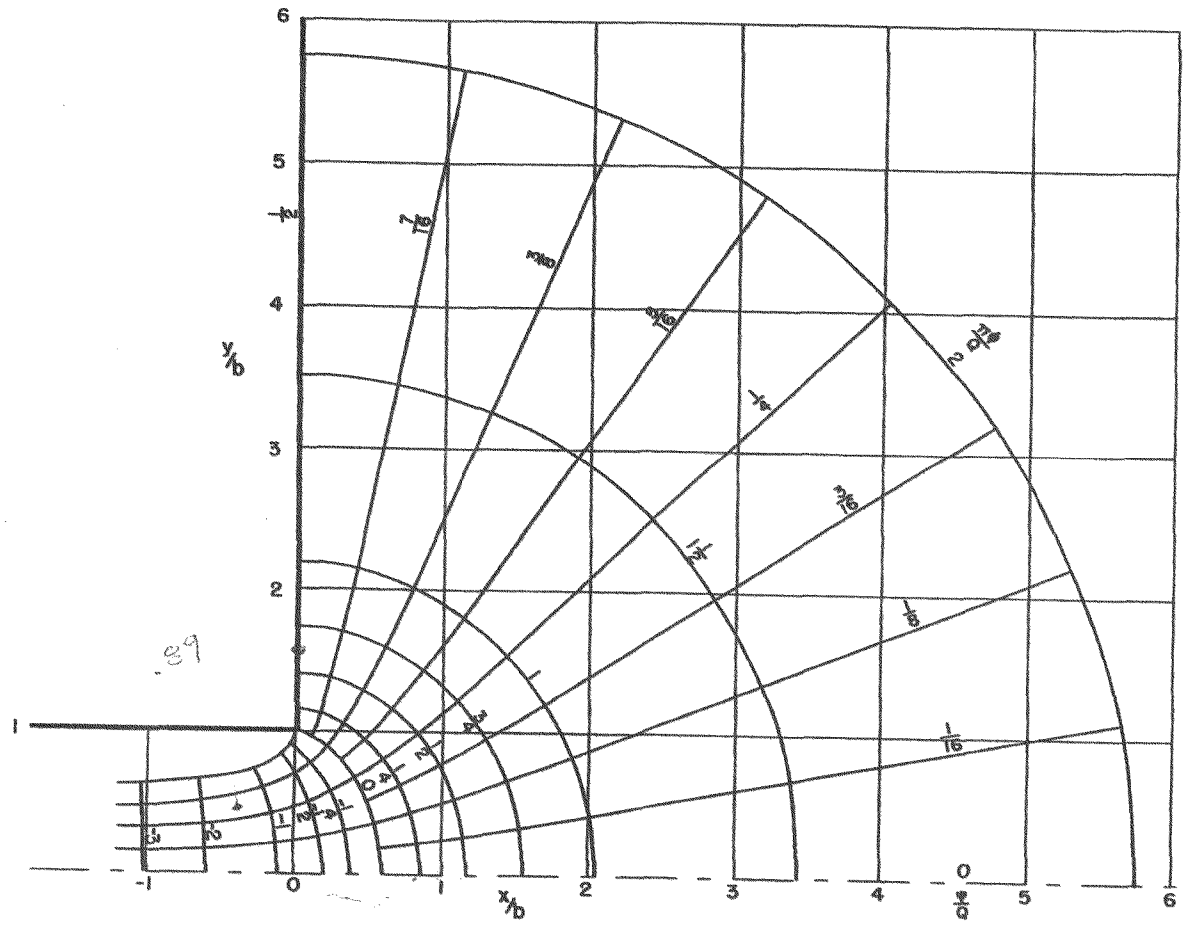

Fig. 5. Flow pattern through two-dimensional orifice

it is more convenient to proceed by means of equation 2, from which, in view of equation 3,

$$\sinh\left[\log\frac{V}{q} + i\theta\right] = e^{\frac{\pi W}{Q}} \tag{13}$$

Substituting for W, its values in terms of ϕ and ψ, and separating reals and imaginaries

$$\sinh \log\frac{V}{q}\cos\theta = e^{\frac{\pi\phi}{Q}}\cos\frac{\pi\psi}{Q} \tag{14}$$

and

$$\cosh \log\frac{V}{q}\sin\theta = e^{\frac{\pi\phi}{Q}}\sin\frac{\pi\psi}{Q} \tag{15}$$

Eliminating θ between equations 14 and 15 and rearranging,

$$\cosh^2 \log \frac{V}{q} = 1/2 \left[e^{\frac{2\pi\phi}{Q}} + 1 \pm \sqrt{\left(e^{\frac{2\pi\phi}{Q}} + 1 \right)^2 - 4e^{\frac{2\pi\phi}{Q}} \sin^2 \frac{\pi\psi}{Q}} \right] \quad (16)$$

Since V/Q must be infinite for $\phi = \infty$, the positive sign before the radical must be used.

32. Through this equation the velocity of any point may be determined in terms of the constant velocity V of the free streamline. In table 2 this has been done for various values of ψ/Q and $\pi\phi/Q$. It is, however, more convenient in many practical applications to express q in terms of the mean velocity in the channel. Letting V_m be the mean channel velocity, we have

$$V_m = \frac{c}{b} V$$

where, as before, c is the half-width of the jet at infinity and b is the half-width of the channel. In view of equation 10,

$$V_m = \frac{\pi}{2 + \pi} V = 0.611 V$$

33. Using this relation and equation 16, values of q/V and q/V_m have been plotted against s/b in fig. 6 where s is the distance measured along a particular streamline from its intersection with the zero potential line. The value of s for any given value of ϕ and ψ was determined from fig. 5.

34. The use of the data of figs. 5 and 6 in determining the horizontal velocity distribution in the approaches to a channel entrance are illustrated by the following example. Suppose the half-width, b, of the channel is 500 ft and the difference in surface elevation between the ocean and lagoon is such that the rate of discharge in the channel, of width $2b$, is 2000 cfs per foot of depth. Suppose further that we wish to determine the velocity at the point $x/b = 0$, $y/b = 0.7$, or in this example for a channel half-width, b, of 500 ft, $x = 0$ and $y = 350$ ft. From

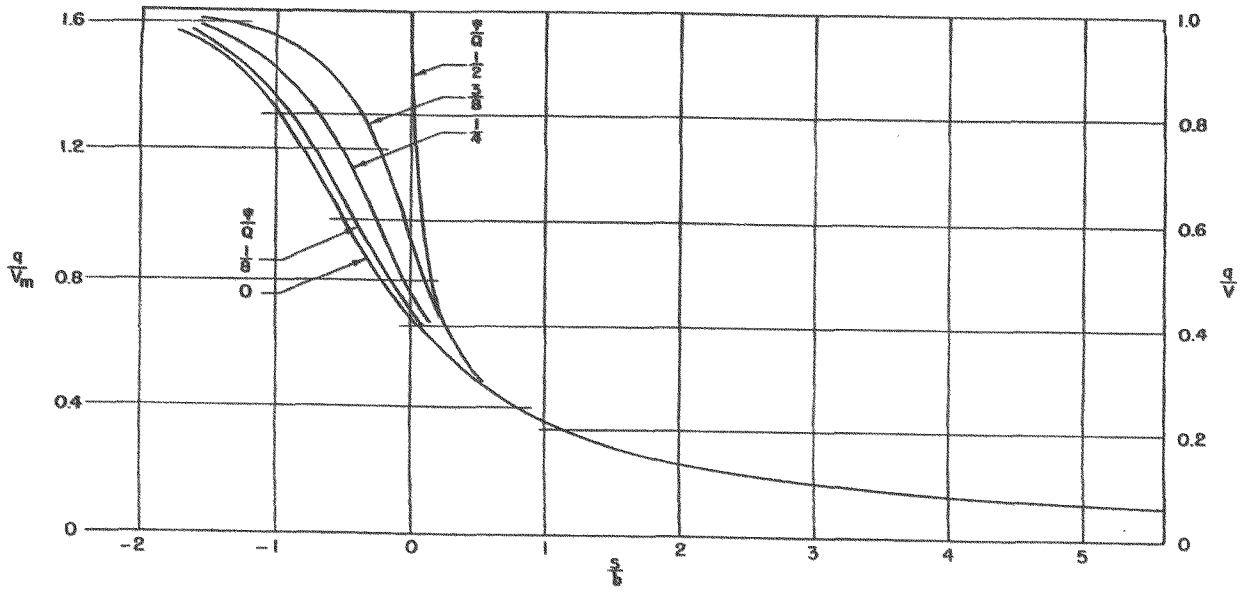

Fig. 6. Variation of velocity along streamlines for flow through two-dimensional orifice

fig. 5 this point is seen to be on the streamline for which $\psi/Q = 3/8$, and using fig. 5, s measured from the zero potential line to the point in question is found to be -0.3b. Referring to the curve for $\psi/Q = 3/8$ in fig. 6, it is found that $q/V_m = 1.26$ for the $s/b = -0.3$. Since $V_m = Q/2b$ we have, using the value of Q and b assigned for this illustration,

$$V_m = 2.00 \text{ ft/sec}$$

Hence at $s/b = -0.3$, on the streamline in question we have

$$q = 1.26\ V_m = 2.52 \text{ ft/sec}$$

35. The direction of the velocity vector will, of course, be tangential to the streamline at the point in question.

36. An example of the application of the generalized solution shown in fig. 5 to a specific assumed condition is given in Appendix A.

37. It is again pointed out that the analysis from which the preceding results are derived is based on the assumption that pure, nonviscous, potential flow obtains, and that the jet shown in fig. 4 is bounded by free streamlines with the region between the free streamlines and the channel

walls being filled with water at rest. In reality the region between the free streamline and the channel wall is in eddying motion, and the lateral diffusion of the eddies as they move downstream causes the jet to spread eventually to the full width of the channel. Under these circumstances, as previously stated, the use of the results herein obtained to determine velocity distributions at appreciable distances downstream from the channel entrance would not be justified.

38. Since the velocity component normal to a streamline is zero, any of the streamlines of fig. 5 may be replaced by a bounding surface without in any way affecting the flow net. In this manner a relatively wide variety of possible channel-entrance conditions may be obtained from fig. 5. In this connection it is obvious that the relative magnitudes of the mean velocity V_m in the channel, and V the velocity along the free streamline, and also the velocity of the jet at relatively large distances from the channel entrance depend on the type of channel entrance assumed. For example, with the channel width being assumed equal to the full width of the two-dimensional orifice, $V_m = 0.611\ V$ as we have seen. However, if we replace the free streamline with a fixed boundary, $c = b$ and $V_m = V$. Obviously the values of q/V_m given in fig. 6 apply only to the case of the channel shown in fig. 5.

39. Since the free streamlines approach asymptotically the line $y/b = 0.611$, the channel formed by replacing the free streamlines by a fixed boundary will not, strictly speaking, consist of a channel with straight parallel walls. However, it is apparent from fig. 5 that the free streamlines approach the value $y/b = 0.611$ so rapidly for small values of x/b that a channel consisting of straight parallel walls beyond $x/b = -1$, and with the walls coinciding with the free streamlines from $x/b = -1$ to $x/b = 0$, may for all practical purposes be considered to follow the free streamlines throughout their length.

40. The modification in the method of computing the velocity at any point by replacing a streamline of fig. 5 by a fixed boundary is obvious. For example, to continue the illustration of replacing the free streamline with a bounding surface, we see from fig. 6 that $q/V = 0.77$ at the point on the streamline $\psi/Q = 3/8$ for which $s/b = -0.3$.

41. Since $V = V_m = Q/2b$ in this case, using the values of the previous illustration, we have

$$V = 1000/500 = 2.0 \text{ ft/sec}$$

and

$$q = 0.77\ V = 1.54 \text{ ft/sec}$$

42. If both boundaries of the flow are taken to be streamlines in the interior of the jet, it is again evident from fig. 5 that a channel with parallel straight walls for $x/b < -1$ and following the streamlines in question for $s/b > -1$ closely approximates the theoretical configuration, and that again as for the case of the free streamline being replaced by a fixed wall, c is to a close approximation equal to b, and likewise from a consideration of fig. 6 it is evident that V_m may with small error be taken as V. Hence, values of q/v shown in fig. 6 may be used to obtain the velocity at any point in the field of flow when the channel and entrance are such that the boundary walls consist of straight parallel walls up to $x/b = -1$ and coincide with streamlines as x/b increases in the positive direction.

43. It will be noted in fig. 5 that the stream function ψ has been expressed in terms of Q, the discharge per unit depth of channel. This appears logical since it is a characteristic of the stream function that the difference between its value at any two points represents the volume rate of flow per unit depth across any line joining the two points. However, the stream function may be expressed equally well in other forms. For example, since $Q = 2\ Vc$, and using equation 10, the lines of constant ψ may be conveniently represented by $\psi/vb = \gamma$, where γ is a dimensionless number.

Long parallel jetties extending into ocean from the channel entrance

44. This type of entrance condition corresponds essentially to the two-dimensional form of Borda's mouthpiece--the longer the jetties, the closer the correspondence.

45. In fig. 7 is shown the geometry of the channel entrance. The subscript ∞ on some of the points is used to indicate that the point is located at infinity. As before, Q is the discharge into the channel per unit depth of channel, b is the half-width of the channel, and the streamlines will be denoted in terms of the discharge per unit depth of channel. Thus, the streamline along the boundary B'_∞, A', C'_∞ being $\psi = -Q/2$ and the upper bounding streamline being $\psi = Q/2$, the zero streamline is coincident with the x-axis.

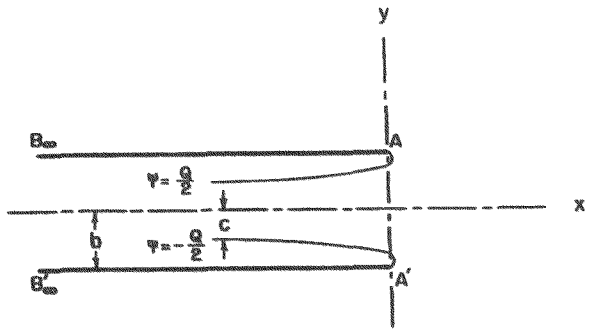

Fig. 7. Channel entrance corresponding to long parallel jetties extending into ocean

46. Milne-Thompson (page 283 of reference 6), proceeding by the usual methods of conformal transformations, derives the solution

$$-V \frac{dz}{dW} = \left[t + \sqrt{t^2 - 1}\right]^2 \tag{17}$$

$$W = \frac{2 \sigma bV}{\pi} \log t - i \sigma bV \tag{18}$$

where t is a complex parameter; b is the half-width of the channel as shown in fig. 7; σ is the coefficient of contraction; and V is, as before, the velocity along the free streamline. Obviously Q, the discharge per unit depth in the channel, is equivalent to the term $2 \sigma bV$ and equation 18 becomes

$$W = \frac{Q}{\pi} \log t - i \frac{Q}{2} \tag{19}$$

from which

$$t = e^{\frac{W\pi}{Q} + \frac{i\pi}{2}} = ie^{\frac{W\pi}{Q}} \tag{20}$$

Substituting the above relation in equation 17

$$V \frac{dz}{dW} = \left[e^{\frac{W\pi}{Q}} + \sqrt{e^{\frac{2W\pi}{Q}} + 1}\right]^2 \tag{21}$$

Integrating this expression,

$$Vz = \frac{Q}{\pi} e^{\frac{2\pi W}{Q}} + \frac{Q}{\pi} e^{\frac{\pi W}{Q}} \sqrt{e^{\frac{2\pi W}{Q}} + 1} + \frac{Q}{\pi} \log \left[e^{\frac{\pi W}{Q}} + \sqrt{e^{\frac{2\pi W}{Q}} + 1} \right] + W + A \qquad (22)$$

where A may be a complex constant. In order to evaluate A we have, since in the development of equation 18 the potential ϕ was assumed to be zero at A and A',

$$\text{at } z = ib, \; W = iQ/2$$

$$\text{at } z = -ib, \; W = -iQ/2$$

The application of the first condition to equation 22 yields

$$A = iVb - iQ + Q/\pi \qquad (23)$$

and the second condition gives

$$A = -iVb + iQ + Q/\pi \qquad (24)$$

Hence $A = Q/\pi$ and equation 22 becomes

$$Vz = \frac{Q}{\pi} e^{\frac{2\pi W}{Q}} + \frac{Q}{\pi} e^{\frac{\pi W}{Q}} \sqrt{e^{\frac{2\pi W}{Q}} + 1} + \frac{Q}{\pi} \log \left[e^{\frac{\pi W}{Q}} + \sqrt{e^{\frac{2\pi W}{Q}} + 1} \right] + W + \frac{Q}{\pi} \qquad (25)$$

From equations 23 and 24 it is clear also that

$$Vb = Q \qquad (26)$$

and since $Q = 2cV$, where c is the half-width of the jet at infinity, it follows that the coefficient of contraction

$$\sigma = c/b = 1/2$$

in accordance with the usual result.

47. In order to compute the streamlines from equation 25, it is necessary to separate the real and imaginary parts of the expression. In this connection the terms under the radical signs offer the only difficulty. These terms may be expanded in a binomial series as in the preceding section, or they may be evaluated directly in the usual manner as follows. Consider first the term

$$\sqrt{e^{\frac{2\pi W}{Q}} + 1}$$

appearing in the right-hand side of equation 25. We may write

$$\sqrt{e^{\frac{2\pi W}{Q}} + 1} = \sqrt{\left(1 + e^{\frac{2\pi W}{Q}} \cos \frac{2\pi\psi}{Q}\right) + ie^{\frac{2\pi W}{Q}} \sin \frac{2\pi\psi}{Q}}$$

Placing the right-hand member of this relation in polar form, and rearranging, we have for positive values of the stream function

$$\sqrt{e^{\frac{2\pi W}{Q}} + 1} = \sqrt{\frac{\left(1 + 2e^{\frac{2\pi\phi}{Q}} \cos \frac{2\pi\psi}{Q} + e^{\frac{4\pi\phi}{Q}}\right)^{1/2} + 1 + e^{\frac{2\pi\phi}{Q}} \cos \frac{2\pi\psi}{Q}}{2}} + i\sqrt{\frac{\left(1 + 2e^{\frac{2\pi\phi}{Q}} \cos \frac{2\pi\psi}{Q} + e^{\frac{4\pi\phi}{Q}}\right)^{1/2} - 1 - e^{\frac{2\pi\phi}{Q}} \cos \frac{2\pi\psi}{Q}}{2}} \qquad (27)$$

Since the term in parentheses under the radical will always be real, equation 27 may be used to determine the real and imaginary parts of

$$\sqrt{e^{\frac{2\pi W}{Q}} + 1}$$

and we may write

$$\sqrt{e^{\frac{2\pi W}{Q}} + 1} = \alpha + i\beta \qquad (28)$$

where α and β represent the real and imaginary portions, respectively, of the expression under the radical, as computed by means of equation 27.

48. In like manner it follows that

$$e^{\frac{\pi W}{Q}}\sqrt{e^{\frac{2\pi W}{Q}}+1}=\left[\alpha\, e^{\frac{\pi\phi}{Q}}\cos\frac{\pi\psi}{Q}-\beta\, e^{\frac{\pi\phi}{Q}}\sin\frac{\pi\psi}{Q}\right]+$$

$$i\left[\alpha\, e^{\frac{\pi\phi}{Q}}\sin\frac{\pi\psi}{Q}+\beta\, e^{\frac{\pi\phi}{Q}}\cos\frac{\pi\psi}{Q}\right] \qquad (29)$$

Letting

$$\alpha_1=\alpha\, e^{\frac{\pi\phi}{Q}}\cos\frac{\pi\psi}{Q}-\beta\, e^{\frac{\pi\phi}{Q}}\sin\frac{\pi\psi}{Q} \qquad (30)$$

and

$$\beta_1=\alpha\, e^{\frac{\pi\phi}{Q}}\sin\frac{\pi\psi}{Q}+\beta\, e^{\frac{\pi\phi}{Q}}\cos\frac{\pi\psi}{Q} \qquad (31)$$

we have from equation 29

$$e^{\frac{\pi W}{Q}}\sqrt{e^{\frac{2\pi W}{Q}}+1}=\alpha_1+i\,\beta_1 \qquad (32)$$

For the expression in brackets appearing in equation 25 we may write

$$e^{\frac{\pi W}{Q}}+\sqrt{e^{\frac{2\pi W}{Q}}+1}=e^{\frac{\pi\phi}{Q}}\cos\frac{\pi\psi}{Q}+\alpha+i\left[e^{\frac{\pi\phi}{Q}}\sin\frac{\pi\psi}{Q}+\beta\right]$$

and letting

$$\alpha_2=e^{\frac{\pi\phi}{Q}}\cos\frac{\pi\psi}{Q}+\alpha \qquad (33)$$

and

$$\beta_2=e^{\frac{\pi\phi}{Q}}\sin\frac{\pi\psi}{Q}+\beta \qquad (34)$$

we have

$$e^{\frac{\pi W}{Q}}+\sqrt{e^{\frac{2\pi W}{Q}}+1}=\alpha_2+i\,\beta_2 \qquad (35)$$

from which

$$\log\left[e^{\frac{\pi W}{Q}} + \sqrt{e^{\frac{2\pi W}{Q}} + 1}\right] = \log\sqrt{\alpha_2^2 + \beta_2^2} + i\cos^{-1}\frac{\alpha_2}{\sqrt{\alpha_2^2 + \beta_2^2}} \qquad (36)$$

Hence, using equations 28, 32, and 36, we may write for equation 25

$$z = \frac{Q}{\pi V} e^{\frac{2\pi\phi}{Q}} \cos\frac{2\pi\psi}{Q} + \frac{Q}{\pi V}\alpha_1 + \frac{Q}{\pi V}\log\sqrt{\alpha_2^2 + \beta_2^2} + \frac{\phi}{V} + \frac{Q}{\pi V} +$$

$$i\left[\frac{Q}{\pi V} e^{\frac{2\pi\phi}{Q}} \sin\frac{2\pi\psi}{Q} + \frac{Q}{\pi V}\beta_1 + \frac{Q}{\pi V}\cos^{-1}\frac{\alpha_2}{\sqrt{\alpha_2^2 + \beta_2^2}} + \frac{\psi}{V}\right] \qquad (37)$$

49. Separating reals and imaginaries,

$$x = \frac{Q}{\pi V} e^{\frac{2\pi\phi}{Q}} \cos\frac{2\pi\psi}{Q} + \frac{Q}{\pi V}\alpha_1 + \frac{Q}{\pi V}\log\sqrt{\alpha_2^2 + \beta_2^2} + \frac{\phi}{V} + \frac{Q}{\pi V} \qquad (38)$$

and

$$y = \frac{Q}{\pi V} e^{\frac{2\pi\phi}{Q}} \sin\frac{2\pi\psi}{Q} + \frac{Q}{\pi V}\beta_1 + \frac{Q}{\pi V}\cos^{-1}\frac{\alpha_2}{\sqrt{\alpha_2^2 + \beta_2^2}} + \frac{\psi}{V} \qquad (39)$$

Expressing ϕ and ψ in terms of Q, the rate of discharge per unit depth through the channel,

$$\frac{\pi\phi}{Q} = \gamma_1 \qquad (40)$$

$$\frac{\psi}{Q} = \gamma_2 \qquad (41)$$

where γ_1 and γ_2 are pure numbers. Using equations 26, 40, and 41, equations 38 and 39 become

$$\frac{x}{b} = \frac{e^{2\gamma_1}}{\pi}\cos 2\pi\gamma_2 + \frac{\alpha_1}{\pi} + \frac{1}{\pi}\log\sqrt{\alpha_2^2 + \beta_2^2} + \frac{\gamma_1 + 1}{\pi} \qquad (42)$$

and

$$\frac{y}{b} = \frac{e^{2\gamma_1}}{\pi} \sin 2\pi\gamma_2 + \frac{\beta_1}{\pi} + \frac{1}{\pi} \cos^{-1} \frac{\alpha_2}{\sqrt{\alpha_2^2 + \beta_2^2}} + \gamma_2 \qquad (43)$$

50. The two relations above may be used to determine the equipotential lines and streamlines of the flow pattern in the z plane. In table 3, values of x/b and y/b corresponding to various values of ψ/Q and $\pi\phi/Q$ have been computed; and in fig. 8 these data have been used to plot the flow net for the upper half of the channel. Since the flow is symmetrical about the channel axis, the flow net in the lower half will be identical.

51. The determination of the velocities at any point in the channel or in the approaches to the channel may be made in a manner similar to that employed in the preceding section. From equation 21, we have in view of equation 2,

$$-\frac{V}{q} e^{i\theta} = \left[e^{\frac{W\pi}{Q}} + \sqrt{e^{\frac{2W\pi}{Q}} + 1} \right]^2 \qquad (44)$$

and using equation 32 we may write

$$-\frac{V}{q} (\cos\theta + i \sin\theta) = 2e^{\frac{2\pi\phi}{Q}} \left(\cos\frac{2\pi\psi}{Q} + i \sin\frac{2\pi\psi}{Q}\right) + 2\alpha_1 + 2i\beta_1 + 1$$

from which

$$-\frac{V}{q} \cos\theta = 2e^{\frac{2\pi\phi}{Q}} \cos\frac{2\pi\psi}{Q} + 2\alpha_1 + 1 \qquad (45)$$

$$-\frac{V}{q} \sin\theta = 2e^{\frac{2\pi\phi}{Q}} \sin\frac{2\pi\psi}{Q} + 2\beta_1 \qquad (46)$$

and eliminating θ

$$\frac{V^2}{q^2} = 4 e^{\frac{4\pi\phi}{Q}} + 4(2\alpha_1 + 1) e^{\frac{2\pi\phi}{Q}} \cos\frac{2\pi\psi}{Q} + (2\alpha_1 + 1)^2 +$$

$$8\beta_1 e^{\frac{2\pi\phi}{Q}} \sin\frac{2\pi\psi}{Q} + 4\beta_1^2 \qquad (47)$$

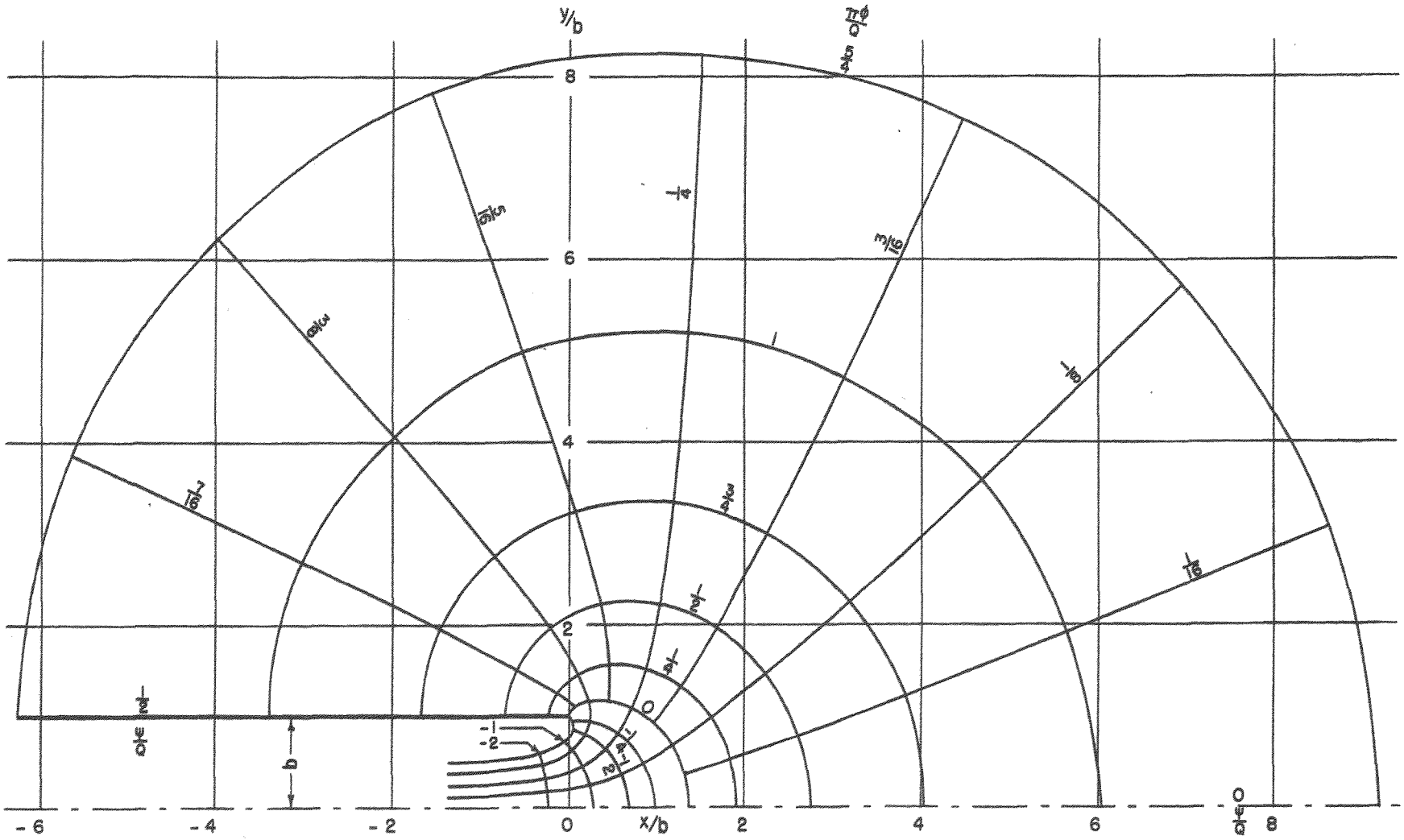

Fig. 8. Flow pattern for long parallel jetties extending into ocean from the channel entrance

52. The preceding relation was used together with the data of fig. 8 to plot q/V against s/b in fig. 9 for several of the streamlines, where as

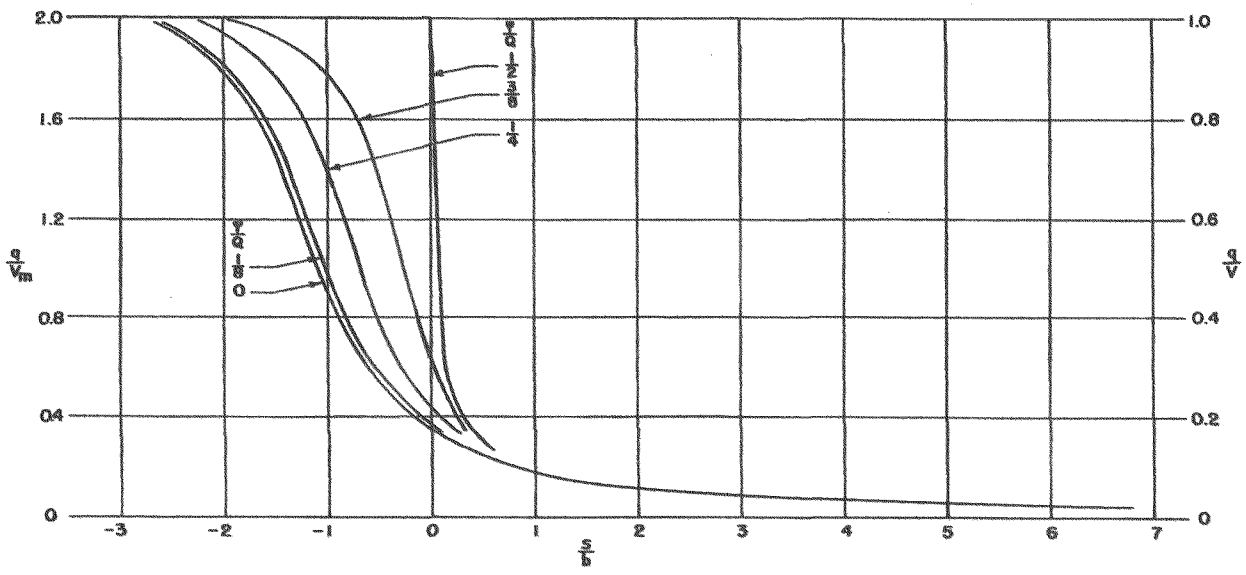

Fig. 9. Variation of velocity along streamlines for the case of long parallel jetties extending into the ocean from the channel entrance

before s is the distance along the streamline measured from its intersection with the zero potential line. In table 4, computed values of q/V and measured values of s/b obtained from fig. 8 are given. The data of figs. 8 and 9 make it possible to compute the magnitude and direction of the velocity at any point in the field of flow.

53. It may again be noted that in the analysis leading to equations 17 and 18, pure potential flow of a nonviscous fluid was assumed. In particular, as previously pointed out, the theory assumes that an abrupt discontinuity in velocity occurs at the free streamline and that the area between the jet and the boundary is occupied by liquid at rest. Owing to viscosity, this assumption obviously introduces an approximation, and the space between the jet and the boundary wall downstream from the channel entrance will be occupied, of course, by an eddy with the jet expanding some distance downstream to the full width of the channel. Under these circumstances the use of the theory for determining velocities at points a substantial distance downstream from the channel entrance is not warranted.

54. As previously pointed out, any streamline in fig. 8 may be

replaced by a fixed boundary without in any way affecting the flow pattern. For this reason the velocity distribution for a relatively wide variety of possible channel-entrance shapes may be obtained from figs. 8 and 9.

Status of Problem

55. In this part (I), the flow patterns for two shapes of channel entrances have been computed. Inasmuch as any of the streamlines may be replaced by fixed boundaries without affecting the flow pattern, it is possible from the data given to approximate several other shapes of channel entrances. It is nevertheless regretted that the flow net for other possible types of channel entrances could not be determined because of time limitations. This is particularly true with respect to the channel-entrance shapes shown in figs. 2(a) and 2(d) and also with respect to a solution given by Michell[5] which corresponds to the effect of a littoral current on the flow through an aperture in a plane wall.

56. The ability of the data given to determine approximately the velocity distribution in the approaches to an actual channel entrance has not been investigated. In this connection the U. S. Coast and Geodetic Survey[8] has in recent years published material on the tidal currents in many of the principal harbors of the country. This material has not yet been examined in detail. If examination of the Coast and Geodetic Survey data should indicate its suitability for this purpose, one of the subsequent progress reports of this project will apply the material given herein to an appropriate channel entrance covered by the Coast and Geodetic Survey investigations.

57. In this same connection it may be observed that the boundary contours of a natural channel entrance will in general never conform precisely to the simple shapes assumed herein or indeed to any other theoretical investigation. The degree of approximation introduced thereby will ordinarily be, at best, of the same order of magnitude as that introduced by the application of uniform-flow formulas to the flow of natural rivers. Under these circumstances, the degree of refinement warranted in theoretical considerations of the problem is open to question. Nevertheless, it is believed that the extension of the present investigation to

the determination of the velocity distributions in some of the more complicated channel-entrance shapes, such as those of figs. 2 and 3, would be fully warranted.

References

1. Cisotti, Umberto, Idromeccanica Piana. Milano, 1921.

2. Greenhill, Theory of a Streamline Past a Plane Barrier. Reports and Memoranda No. 19, Advisory Committee for Aeronautics, London, 1910.

3. _____, Theory of a Streamline Past a Curved Wing. Appendix to Report No. 19, Advisory Committee for Aeronautics, London, 1916.

4. Lamb, Horace, Hydrodynamics. Dover, New York, 1945.

5. Michell, J. H., "On the theory of free stream-lines." Phil. Trans., A, vol 181 (1890).

6. Milne-Thompson, Louis Melville, Theoretical Hydrodynamics. The Macmillan Company, New York, 1950.

7. Prasil, F., Technische Hydrodynamik. 2d ed., Julius Springer, Berlin, 1926.

8. U. S. Coast and Geodetic Survey, Special Publications:

   No. 111, Rev (1935) ed., Tides and Currents in New York Harbor, by H. A. Marmer.
   No. 115, Tides and Currents in New York, by L. P. Disney.
   No. 123, Tides and Currents in Delaware Bay, by L. M. Zeskind.
   No. 127, Tides and Currents in S. E. Alaska, by R. A. Woodworth and F. J. Haight. 1927.

9. Von Mises, "Berechnung von Ausfluss und Ueberfallzahlen." Zeitschrift des Vereines Deutscher Ingenieure, vol 61, Nos. 21, 22, and 23 (1917), pp 447-452, 469-474, 493-498.

PART II: THE VELOCITY DISTRIBUTION IN THE JET ISSUING FROM A CHANNEL INTO AN OCEAN OR LAGOON

Introduction

58. In Part I of this report, the velocity distribution in the approaches to a channel entrance was considered for the case of flow from the ocean or lagoon into the channel entrance. In Part II, the reverse problem will be considered. That is, the velocity distribution in the approaches to the channel entrance will be investigated for the case of flow from the channel into the quiet water of the ocean or lagoon.

59. A schematic sketch of the problem is shown in fig. 10. In the figure as drawn, it is assumed that the tidal fluctuation in the ocean at the time of observation is such that flow is from the lagoon into the channel and thence to the ocean. Owing to turbulent mixing of the high-velocity channel flow with the surrounding quiet water, the jet issuing from the channel into the ocean spreads laterally, with a consequent decrease in velocity. If the ocean depth at the channel entrance is greater than the depth of the channel, or if the ocean depth increases with distance away from the channel entrance, the processes of turbulent diffusion will cause the jet to spread vertically from the channel entrance toward the ocean bottom. The complexity of this three-dimensional problem is such that it is not amenable to simple analysis, and for convenience the present investigation will be restricted to those situations in which the bottom of the channel and ocean are such that to an approximation, at least, the flow may be considered essentially two-dimensional.

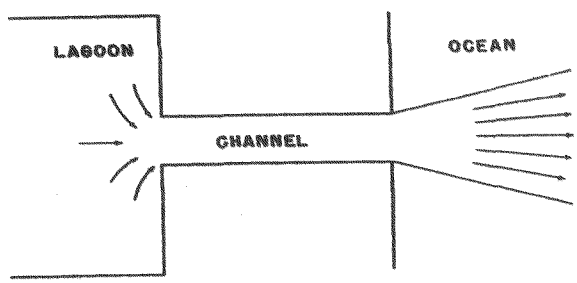

Fig. 10. Definition sketch of problem

Statement of Problem

60. Tollmien[10*] was the first to investigate theoretically the turbulent diffusion of two-dimensional jets. Tollmien's analysis was based on the momentum-transport theory of turbulence. Later investigators have (a) modified Tollmien's momentum-transfer methods somewhat to secure better conformance with experiment[8]; (b) used the method of vorticity transport to determine the velocity distribution in the jet[6]; or (c) have proceeded entirely on the basis of general momentum and energy considerations, with the use of the error function, to represent the velocity distribution.[1]

61. With suitable choice of constants, both the momentum- and vorticity-transfer theories yield velocity distributions in close agreement with experiment.

62. The velocity in the jet is also closely approximated by the error function; the use of the error function for this purpose has the advantage of simplicity, but it is not based on any particular theory of turbulence diffusion.

63. The velocity distributions of Tollmien's jet analysis agree closely with experiment, and in lieu of a more satisfactory theory of jet diffusion, the results of Tollmien's investigation will be used for the present problem of the turbulent diffusion of two-dimensional jets. In this connection, Tollmien studied two aspects of the problem. The first was the free jet boundary, shown schematically in fig. 11, in which the turbulent mixing along the boundary between a stream of uniform velocity and adjacent still fluid is investigated. The second aspect of the two-dimensional jet problem studied by Tollmien was the case of jet efflux from a linear slot in a plane wall, such as shown in fig. 12.

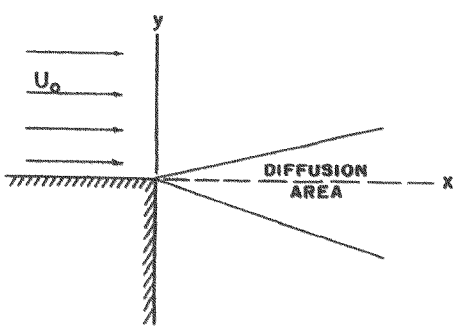

Fig. 11. Definition sketch of free jet boundary

64. These two concepts of the physical phenomena involved in the turbulent diffusion of jets may be applied readily to the

* Raised numbers refer to references at the end of this part (Part II).

detailed mixing processes observed with a jet flowing from a slot of definite width into a region of still fluid. First, as the fluid emerges from the slot of width "a" with uniform velocity, the velocity discontinuity between the jet and the layer of still fluid on either side of the jet generates eddies, which causes a diffusion pattern to be set up along the jet boundary similar to that shown in fig. 11. The lateral mixing process spreads inward into the constant-velocity core of the jet and outward into the surrounding still fluid. Consequently, the width of the constant-velocity core of the jet decreases with distance from the slot as shown in fig. 13, and eventually becomes zero as the mixing process diffuses from both boundaries of the two-dimensional jet to the center line. This region of flow in which the constant-velocity core of the jet is annihilated has been aptly termed the zone of flow establishment by Albertson, Dai, Jensen, and Rouse.[1] This zone corresponds to the first aspect of the problem of free turbulence treated by Tollmien--that is, the turbulent mixing along the boundary between a stream of uniform velocity and adjacent still fluid; and the zone of establishment of the turbulent jet issuing from a slot of definite width as shown in fig. 13 may, as will be indicated later, be considered to be made up of two of the diffusion zones investigated by Tollmien and shown in fig. 11.

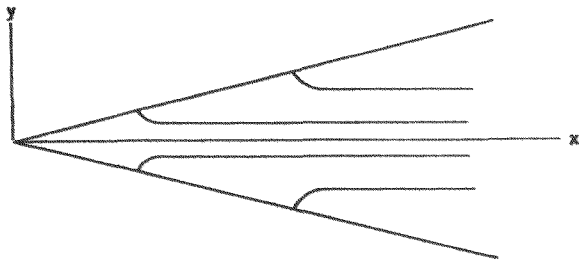

Fig. 12. Definition sketch of Tollmien's jet flow from a linear slot

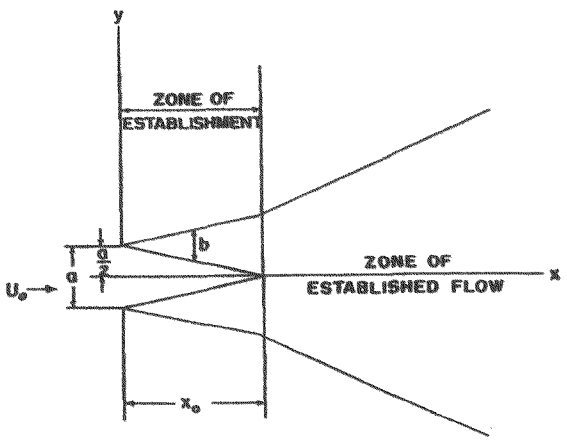

Fig. 13. Jet from a slot of width "a"

65. Beyond the zone of flow establishment the constant-velocity inner core of the jet no longer exists, and the spread of the turbulent mixing process is confined to the outer boundaries of the two-dimensional jet. This region has been termed the zone of established flow by

Albertson, et al.,[1] and corresponds essentially to the second aspect of free turbulence treated by Tollmien--that is, the efflux of a jet from a two-dimensional linear slot.

66. In this part (II), Tollmien's analysis of free turbulence at a plane of velocity discontinuity and his analysis of the lateral diffusion of turbulent mixing for a two-dimensional jet issuing from a linear slot will be applied to the problem of determining the streamlines and computing the velocities in the flow field of a stream of water issuing from a channel into a large body of quiet water such as an ocean.

General Considerations

67. Two-dimensional turbulent-jet theory is amply treated in the literature, and for the purpose of this report there is no need to repeat the detailed argument here. However, as will be seen, certain portions of the theory are necessary for proper application of Tollmien's computed results to the problem treated herein, and for this reason a portion of Tollmien's development, with only minor modifications, will be sketched.

Zone of flow establishment

68. The assumption of similarity of the flow characteristics from section to section of the jet is made in most developments of jet theory, and has been amply verified by experiment. This assumption may be stated thus:

$$\frac{u}{U_o} = f\left(\frac{y}{\beta b}\right) \tag{48}$$

where u is the horizontal component of the velocity, U_o is the velocity in the undisturbed stream of fig. 11, b is the width of the diffusion zone, and β is a constant which may for the moment be considered arbitrary. The origin of the coordinate system is as shown in fig. 11.

69. Tollmien assumed from observation, and Liepman and Laufer[7, p 14] showed analytically that

$$b = \alpha x \tag{49}$$

where α is a constant. The assumption of similarity of flow in the diffusion area thus becomes

$$\frac{u}{U_o} = f(\eta) \qquad \eta = \frac{y}{\zeta x} \tag{50}$$

where $\zeta = \alpha\beta$. The stream function is determined by using equation 50:

$$\psi = \int u dy = U_o \, x \, \zeta F(\eta) \tag{51}$$

where $F(\eta) = \int f(\eta) d\eta$. From the above relation the vertical component of the velocity is determined.

$$v = \frac{\partial \psi}{-\partial x} = -U_o \zeta F(\eta) + U_o \zeta \eta F'(\eta) \tag{52}$$

Tollmien assumed the Prandtl expression for the apparent shear stress, which since $\partial u/\partial y$ is positive for the velocity distributions of fig. 11 is given by

$$\tau = \rho \ell^2 \left(\frac{\partial u}{\partial y}\right)^2 \tag{53}$$

where ρ is the density of the fluid, and ℓ is the mixing length.

70. As Goldstein[4, p 597] has pointed out, it can be shown from the assumption of similarity that ℓ must be proportional to b ; and in like manner it has been noted by both Goldstein and Tollmien[10, p 469] on the basis of the requirement that both sides of the equation of motion

$$u \frac{\partial u}{\partial x} + v \frac{\partial u}{\partial y} = \frac{1}{\rho} \frac{\partial \tau}{\partial y} \tag{54}$$

must vary in the same manner with x , that ℓ must be proportional to x--that is,

$$\ell = cx \tag{55}$$

where c is a constant.

71. Substitution of equations 50, 52, 53, and 55 into equation 54 yields

$$-F(\eta) = \frac{2c^2}{\zeta^3} F'''(\eta) \tag{56}$$

From equation 50, $\zeta = \alpha\beta$, where β is an arbitrary constant. For convenience β may be assigned a value such that

$$\zeta^3 = 2c^2 \tag{57}$$

and equation 56 becomes

$$F(\eta) + F'''(\eta) = 0 \tag{58}$$

which is the differential equation derived by Tollmien.

72. The boundary conditions follow from the fact that at the upper boundary of the diffusion area of fig. 11, $u = U_o$ and $\partial u/\partial y = 0$, and at the lower boundary $u = 0$ and $\partial u/\partial y = 0$. Letting η_1 be the value of η along the upper boundary, and η_2 the value of η along the lower boundary, it follows that

$$\begin{aligned} F(\eta_1) &= \eta_1 \\ F'(\eta_1) &= 1 \\ F''(\eta_1) &= 0 \\ F'(\eta_2) &= 0 \\ \text{and } F''(\eta_2) &= 0 \end{aligned} \tag{59}$$

73. Equation 58, with the boundary conditions of equation 59, has been solved by Tollmien, and the results are shown in table 5.

74. In Tollmien's solution of the jet boundary problem of fig. 11, the constant-velocity stream, as is evident from the boundary conditions of equation 59, is assumed to be unaffected by the turbulent mixing process for values of η greater than η_1. Hence the assumption that the zone of flow establishment of fig. 13 consists of a constant-velocity inner core with a diffusion zone on either side corresponding to Tollmien's problem appears to be warranted.

Zone of established flow

75. The problem of two-dimensional efflux from a linear slot was solved by Tollmien in a manner similar to his solution for the jet boundary. As before, the assumption of similarity of flow from section to section of the jet is made. Equation 49 has been shown by Liepman and Laufer[7, p 12] to be valid for the zone of established flow as well as for the jet boundary, and hence the condition of similarity becomes

$$\frac{u}{U_{max}} = f(\eta) \qquad \eta = \frac{y}{\zeta x} \tag{60}$$

76. Letting $U_{max} = U_o$ for $x = x_o$, it follows directly from equation 60 and the momentum equation,

$$\left[\int_{-\infty}^{\infty} u^2 dy\right] x = x_o = \int_{-\infty}^{\infty} u^2 dy \tag{61}$$

that $U_o^2 x_o = U_{max}^2 x$ and equation 60 then becomes

$$\frac{u}{U_o} = \sqrt{\frac{x_o}{x}}\, f(\eta) = \sqrt{\frac{x_o}{x}}\, F'(\eta) \tag{62}$$

where $F'(\eta) = f(\eta)$.

77. From equation 62 the stream function is determined to be

$$\psi = \int_o^y u dy = U_o \sqrt{x_o}\sqrt{x}\, \zeta F(\eta) \tag{63}$$

and

$$v = \frac{-\partial\psi}{\partial x} = -\zeta U_o \sqrt{\frac{x_o}{x}} \left[\frac{F(\eta)}{2} - \eta F'(\eta)\right] \tag{64}$$

Referring to fig. 12, it is apparent for the upper half of the jet where η is positive that $\partial u/\partial y$ is negative and hence:

$$\tau = -\rho\, \ell^2 \left(\frac{\partial u}{\partial y}\right)^2 \tag{65}$$

78. As with the jet boundary, ℓ must be proportional to b and x, and substituting equations 55, 62, 64, and 65 into the equation of motion, equation 54, and letting as before $\zeta^3 = 2c^2$, we have

$$\left[F'(\eta)\right]^2 + F(\eta)F''(\eta) = 2F''(\eta)F'''(\eta) \tag{66}$$

and direct integration with respect to η yields

$$F'(\eta)F(\eta) = \left[F''(\eta)\right]^2 \tag{67}$$

which is the differential equation of Tollmien.

79. The boundary conditions follow from the fact that at $\eta = 0$, $u = U_{max}$ and $v = 0$, and at the boundary for $\eta = \eta_1$, $u = 0$. From which it follows that

$$F'(0) = 1 \qquad F(0) = 0 \qquad \text{and } F'(\eta_1) = 0 \tag{68}$$

80. Equation 67, with the boundary conditions of equation 68, has been solved by Tollmien, and the results are shown in table 5.

Application of Theory

81. Since the appearance of Tollmien's paper in 1926 there have been many experimental investigations of the diffusion of submerged two-dimensional jets. Without exception, insofar as the writer is aware, these investigations have been made with air jets issuing from relatively small slots. Because of the laws of similitude, it is possible to apply these experimental results with confidence to water jets of comparable Reynolds numbers. However, owing to the use of air as the experimental medium and to the use of small slots, the range of Reynolds numbers covered by the experimental data is substantially below that which might prevail in the present problem with channel widths on the order of 100 ft or larger. For this reason it became desirable to establish, from previous experimental work, the effect of Reynolds number on the constant "c" of Tollmien's analysis.

Determination of Tollmien's "c"

82. Zone of established flow. In order to establish the relation of Tollmien's c to the Reynolds number for the zone of established flow, the value of c has been computed from the experimental data of Albertson, Dai, Jensen, and Rouse,[1] Forthmann,[3] and Reichardt.[9] The values of c thus obtained have been plotted in fig. 14 as a function of the Reynolds number $R = U_o a/\nu$. Inasmuch as the first and third references cited above used the normal probability curve rather than Tollmien's theoretical investigation in analyzing their experimental results, it is necessary

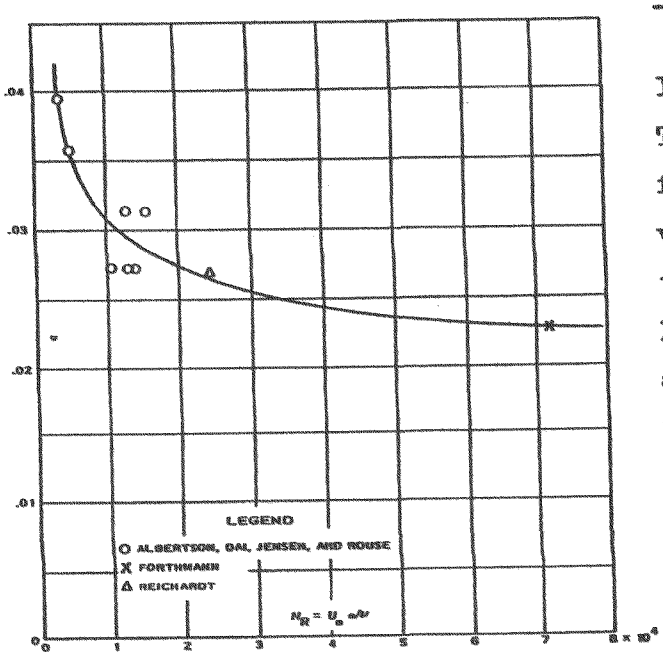

Fig. 14. Variation of the mixing length coefficient "c" with Reynolds number, zone of established flow

to describe the method used in determining Tollmien's c from these experimental data. This is particularly true, since the method used herein is not identical with the method used by Forthmann, the second reference given above. In this connection the measured velocity distribution in two-dimensional jets is such that the measured velocity is greater than that indicated by the Tollmien analysis for velocities near the center line of the jet and lower for velocities near the jet boundaries.

83. Because of this fact the problem of determining Tollmien's c from experimental data involves determining the best fit of various theoretical curves to an experimentally determined curve of a slightly different shape. In order to avoid the indefiniteness inherent in such a process it appeared desirable to define the experimentally determined c as that constant which caused the theoretically determined Tollmien's velocity distribution curve to coincide with the experimentally determined curve at $u/U_{max} = 0.5$. This is a method of evaluating constants pertaining to jet flow that has been used by several investigators.[5,11]

84. In addition, Forthmann, in determining the origin of the idealized two-dimensional jet of fig. 12 with respect to the two-dimensional slot from which the physical jet issues, used a refinement regarding the location of the origin with respect to the slot which somewhat complicates the procedure, and which was not demanded by the accuracy of his experimental work. In order to simplify the procedure of computing Tollmien's c from the various experimental investigations, the origin of the coordinates in which the flow distribution is expressed was taken as the intersection of the center line of the jet with the face of the two-dimensional slot. This procedure for the zone of flow establishment will not produce appreciable error for moderate and great distances from the slot. This method of determining Tollmien's c has the advantage of being simple and definite. In fig. 15, as an illustration, Forthmann's data on the x-component of the velocity has been plotted, together with Tollmien's theoretical curve for $c = 0.0224$ $\left(\sqrt[3]{2c^2} = 0.1\right)$. It will be observed that the experimental and theoretical curves coincide at $u/U_{max} = 0.50$. In connection with the value of c herein determined from Forthmann's data, it is proper to note that Forthmann, on the basis of the same experimental data, determined the value of c to be 0.0165--a value almost identical with

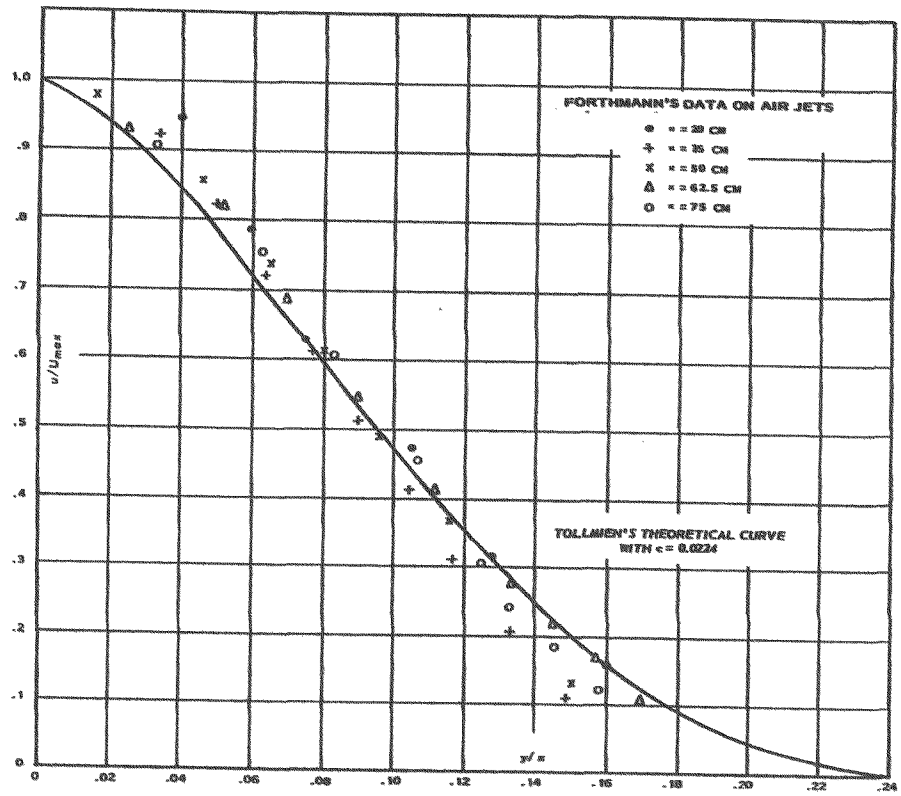

Fig. 15. Forthmann's data on air jets

that determined by Tollmien for the free jet boundary.

85. In fig. 14 the value of Tollmien's c determined from Forthmann's data for the zone of established flow, as well as values of c determined in a similar manner from the data of Reichardt and Albertson et al., have been plotted against the Reynolds number $N_R = U_o a/\nu$. In none of these experimental investigations was the air temperature given, and in computing the Reynolds number of the flow the air temperature was assumed to be 70 F.

86. From fig. 14 it is evident that for small Reynolds numbers, Tollmien's c decreases rapidly with increasing Reynolds number, and as would be expected, it appears that the value of c approaches an asymptotic value as N_R continues to increase to the point where viscous effects become negligible. The data presented in this figure are obviously somewhat fragmentary, and there is appreciable scatter. In particular, the curve for the higher values of the Reynolds number is defined only by the experimental data of Forthmann, and inasmuch as the Reynolds number obtaining with the present problem of flow from a channel into an ocean or

into a lagoon may be on the order of 1000 times greater than those shown in fig. 14, it is apparent, because of gross extrapolation of the existing fragmentary experimental data, that the appropriate value of c for the present problem is somewhat questionable. Nevertheless, from the data of fig. 14 it appears that the value of c approaches asymptotically a value of approximately 0.022 as N_R continues to increase beyond the range of appreciable viscous effect, and it is proposed to use this value of c in applying Tollmien's analysis to the zone of established flow.

87. The need for a systematic experimental investigation over an extended range of Reynolds numbers to define clearly the relation between N_R and c or some other comparable parameter of the jet flow such as x_o is obvious.

88. Zone of establishment. In the zone of establishment, the geometry of which is defined in figs. 11 and 13, there should also be, at least at low Reynolds numbers, a region where viscous effects are appreciable and become apparent. In this connection it may be observed that there is no characteristic constant length to be associated with the geometry of the bounding surfaces of the jet, and therefore, there can be no general Reynolds number defining the flow characteristics, which remains constant throughout the flow pattern. A local Reynolds number based on distance from the two-dimensional slot, width of the diffusion zone, or some other length parameter of the flow must furnish the characteristic length of the flow phenomena for computation of the Reynolds number.

89. In fig. 16 the value c stated by Tollmien[10] and Cordes[2] on the basis of their experimental investigations, together with the value of c computed in the manner described previously, based on the experimental work of Liepman and Laufer,[7] Albertson et al.,[1] and Reichardt,[9] have been plotted against the local Reynolds number $U_o x'/\nu$, where x' is

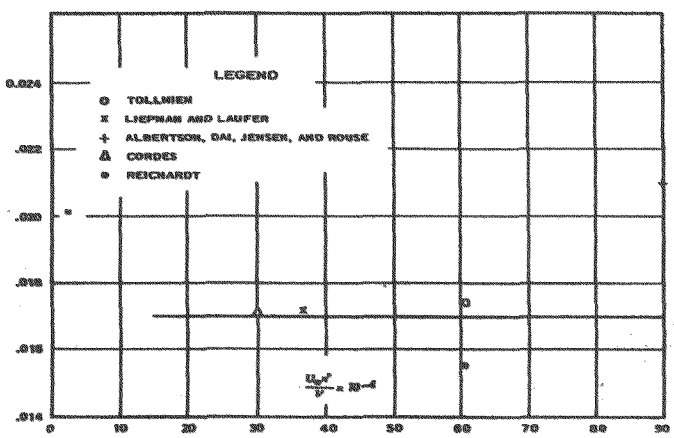

Fig. 16. Variation of Tollmien's c with local Reynolds number at $x' = 1$ ft, zone of flow establishment

the distance from the slot, and for convenience in plotting the data of fig. 16, x' has been taken to be 1 ft. The scatter in the data is such that a precise evaluation of c is impossible, and it appears reasonable to assume that the data of fig. 16 is in the region where the Reynolds number is sufficiently high to make viscous effects negligible and hence to make c independent of Reynolds number. On the basis of the data of fig. 16 it is proposed to use a value of c of 0.017 in the application of Tollmien's results to the zone of establishment.

Determination of streamlines

90. Zone of establishment. The location of the jet streamlines in the zone of establishment may be determined directly from Tollmien's work. From equations 52 and 58,

$$\psi = U_o x \sqrt[3]{2c^2}\, F(\eta) \tag{69}$$

and Tollmien has computed the function $F(\eta)$ for various values of η. These results are shown in table 5.

91. Measuring x in terms of a, the width of the slot, we may write $x = ka$, and substituting in equation 69,

$$\frac{\psi}{kaU_o \sqrt[3]{2c^2}} = F(\eta) \tag{70}$$

Letting $Q = aU_o$, where Q is the volume rate of discharge through the slot per unit depth,

$$\frac{\psi}{kQ \sqrt[3]{2c^2}} = F(\eta) \tag{71}$$

92. From equation 71 and table 5, $k = x/a$ may be computed for given values of ψ/Q, $\sqrt[3]{2c^2}$, and η. Using the value of $\sqrt[3]{2c^2}$ given in the previous section we may determine, from the assumed η, the value of y/a corresponding to the $x/a = k$ and ψ/Q in question. This has been done, and the results have been plotted in fig. 17 to form the streamlines for the zone of establishment. In this connection it is obvious from fig. 13 and the constants regarding jet diffusion determined by Tollmien (table 5) that the length of the zone of flow establishment x_o may be determined from the relation

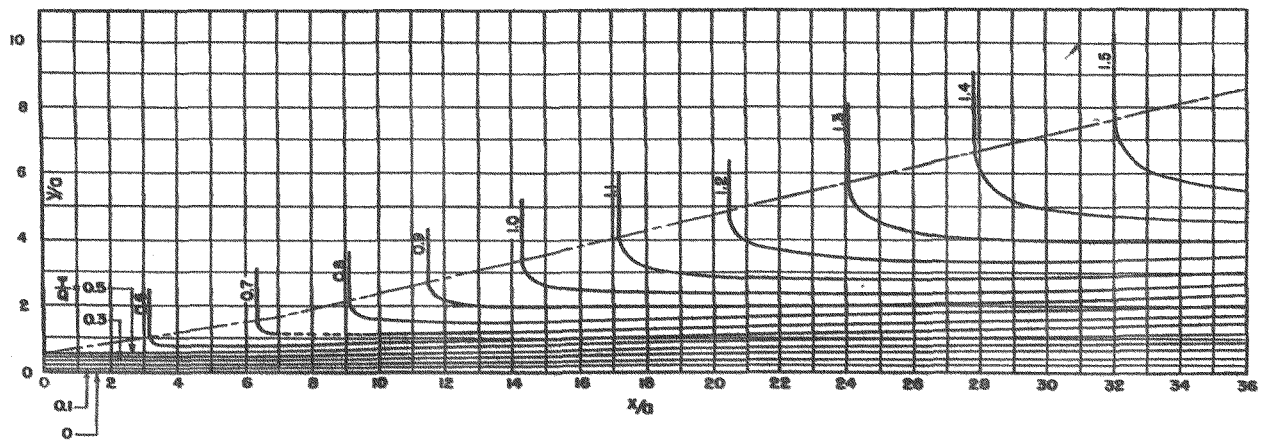

Fig. 17. Streamlines of two-dimensional jet

$$\frac{a}{2} = 0.981 \sqrt[3]{2c^2}\, x_o \tag{72}$$

From which, using the value c = 0.017 previously determined,

$$x_o = 6.12a \tag{73}$$

93. The streamlines in fig. 17, up to a value of x/a = 6.12, have been determined as described above. The streamlines in fig. 17 for values of x/a > 6.12, which corresponds to the zone of established flow, have been determined from Tollmien's analysis for jet efflux from a linear slot.

94. Zone of established flow. By equations 57 and 63,

$$\frac{\psi}{U_o \sqrt{x_o}\sqrt{x}\ \sqrt[3]{2c^2}} = F(\eta) \tag{74}$$

95. The function $F(\eta)$ for the two-dimensional jet issuing from a linear slot has been computed by Tollmien, and the computed values of $F(\eta)$ for various values of η are given in table 5. Expressing the distance from the slot in terms of a, the width of the slot, and letting $Q = aU_o$ as before, equation 74 becomes

$$\frac{\psi}{Q\sqrt{x_o/a}\sqrt{x/a}\ \sqrt[3]{2c^2}} = F(\eta) \tag{75}$$

96. Knowing $F(\eta)$ and η from Tollmien's computations in table 5 and using the value of c = 0.022 or $\sqrt[3]{2c^2} = 0.0989$ from page 33, the values x/a for any streamline may be computed from equation 75. Knowing x/a and η, the corresponding value of y/a may be computed from

$$\frac{y}{a} = \frac{x}{a} \sqrt[3]{2c^2}\, \eta \tag{76}$$

97. At this point it is necessary to point out a difficulty which arises when Tollmien's analyses for the jet boundary of fig. 11 and the two-dimensional jet flow from the linear slot of fig. 12 are used to compute the characteristics of a two-dimensional jet issuing from a slot of definite width. It is obvious that the momentum in the zone of flow establishment must be identical with the momentum in the zone of established flow. Whatever use is made of Tollmien's analyses must be such that this elementary momentum consideration is observed. In fig. 18 is shown the velocity distribution in the two zones of the jet for a value of

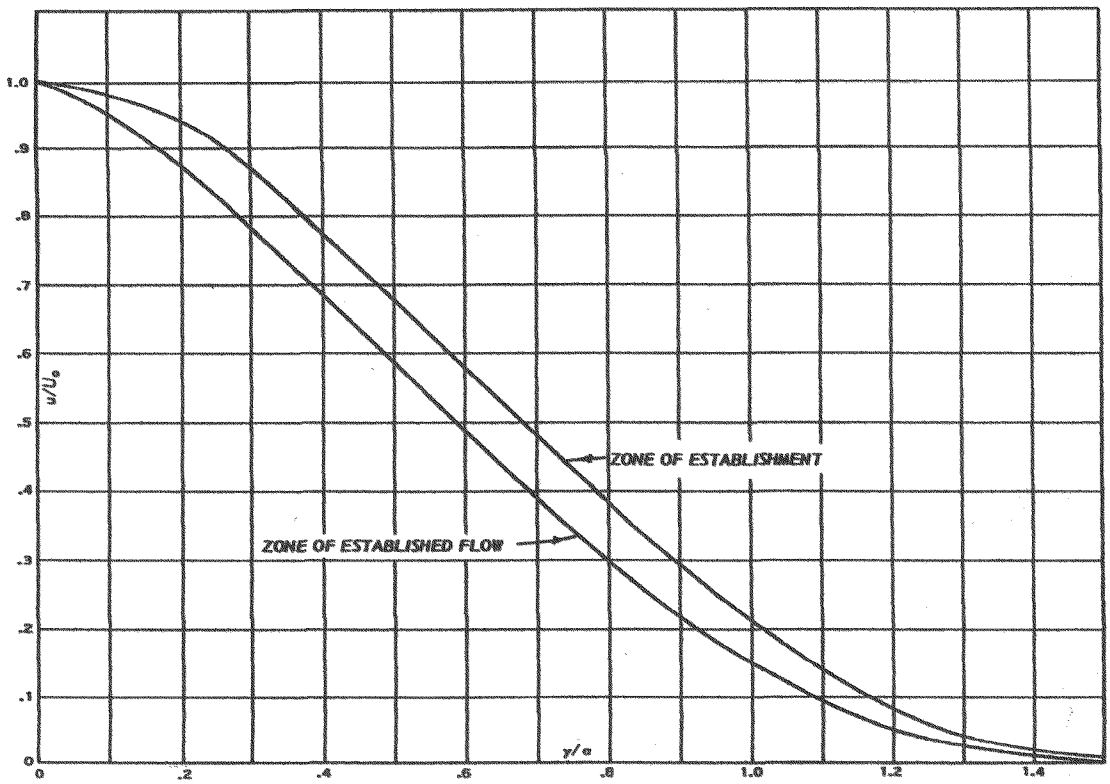

Fig. 18. Velocity distribution at $x = x_o = 6.12a$

$x = x_o = 6.12a$, the nominal limit of the zone of establishment as given in the preceding section.

98. The curve for the zone of established flow in fig. 18 has been computed on the basis that $U_{max} = U_o$ at $x = 6.12a$, and both velocity distribution curves have been computed with the values of c derived in par. 82-87. From this figure it is apparent that the momentum consideration stated above will not hold unless an adjustment of some nature is made. This adjustment may conveniently be made by considering the jet to consist of three zones of flow, instead of the two heretofore mentioned. The first zone would be the zone of flow establishment in which the diffusion of the eddies from the jet boundary steadily expands into the constant-velocity core of the jet until the core is annihilated. The second zone would be the zone of completely established flow, and the third zone would be a transition zone between the first and second in which neither of the analyses of Tollmien would be valid.

99. The condition that the momentum in the zone of established flow be equivalent to that in the zone of flow establishment requires that

$$U_o^2 a = 2\int_0^\infty u^2 dy \tag{77}$$

and since

$$\frac{u}{U_{max}} = f(\eta) = F'(\eta) \qquad \eta = \frac{y}{\sqrt[3]{2c^2}}x \tag{78}$$

we have by equation 77,

$$U_o^2 a = 2x\sqrt[3]{2c^2}\,U_{max}^2\int_0^\infty F'(\eta)d\eta = xU_{max}^2 I \tag{79}$$

where

$$I = 2\sqrt[3]{2c^2}\int_0^\infty F'(\eta)d\eta$$

100. Referring to the idealized jet configuration shown in fig. 13, in which the zone of established flow begins immediately after the zone of flow establishment, it is apparent that at $x = x_o$, $U_{max} = U_o$. Using this fact in equation 79 we have

$$\frac{x_o}{a} = \frac{1}{I} \tag{80}$$

101. The integral I may be evaluated graphically from Tollmien's computations and is found to be 0.1376. Hence

$$\frac{x_o}{a} = \frac{1}{0.1376} = 7.27 \tag{81}$$

102. This is the value of x_o for the zone of established flow required for constancy of momentum in a two-dimensional jet issuing from a slot of width a, whose velocity distribution is that derived by Tollmien for a two-dimensional jet issuing from a linear slot.

103. The value of $x_o/a = 7.27$ derived above for the zone of established flow is to be compared with the value of $x_o/a = 6.12$ derived in the preceding section for the zone of establishment. Since in the derivation of the value of x_o for the zone of established flow it was assumed that $U_{max} = U_o$ at $x = x_o = 7.27a$, while the value of x_o derived for the zone of flow establishment indicates that U_{max} is less than U_o for values of x greater than 6.12a, it is apparent that the velocity distribution developed by Tollmien demands, for constancy of momentum from section to section, the existence of a transition zone between the zone of flow establishment and the zone of established flow.

104. Substituting the value of $x_o/a = 7.27$ obtained above in equation 75, rearranging, and letting $Q = aU_o$, where Q is the volume rate of flow through the slot per unit depth, we have

$$\frac{\psi}{Q} \frac{1}{\sqrt{7.27}\sqrt{x/a}\ \sqrt[3]{2c^2}} = F(\eta) \tag{82}$$

and using the value of $\sqrt[3]{2c^2} = 0.0989$ as previously determined for the zone of established flow,

$$\frac{\psi}{Q} = 0.266\ \sqrt{x/a}\ F(\eta) \tag{83}$$

105. Tollmien has computed $F(\eta)$ for various values of η, and these are given in table 5. Using these values of $F(\eta)$, values of x/a for given values of ψ/Q have been computed from equation 83, and corresponding values

of y/a have been computed from the relation $y/a = x/a \sqrt[3]{2c^2}\ \eta$ and have been plotted in fig. 17.

106. For the streamlines $\psi/Q = 0$ to $\psi/Q = 0.5$, there is very close agreement at the section $x_o = 6.12a$ between the streamlines computed for the zone of establishment and the zone of established flow. The divergence between the streamlines computed for the two zones is more marked for the streamlines $\psi/Q = 0.6$ and 0.7, and as will be noted from fig. 17, portions of these streamlines consist of a dashed line indicating that interpolation was necessary.

107. With regard to the streamline $\psi/Q = 0.7$, its intersection with the jet boundary is dictated by the lateral velocity distribution along the jet boundary. From table 5, the velocity of inflow across the jet boundary for the zone of establishment is

$$\frac{v}{U_o} = 0.379 \sqrt[3]{2c^2} = 0.0316 \qquad (84)$$

108. In like manner from table 5 the velocity of inflow across the jet boundary in the zone of established flow is

$$\frac{v}{U_o} = -0.498 \sqrt{x_o/x} \sqrt[3]{2c^2} = -\frac{0.132}{\sqrt{x/a}} \qquad (85)$$

In fig. 19, equations 84 and 85 have been used to plot the solid portion of

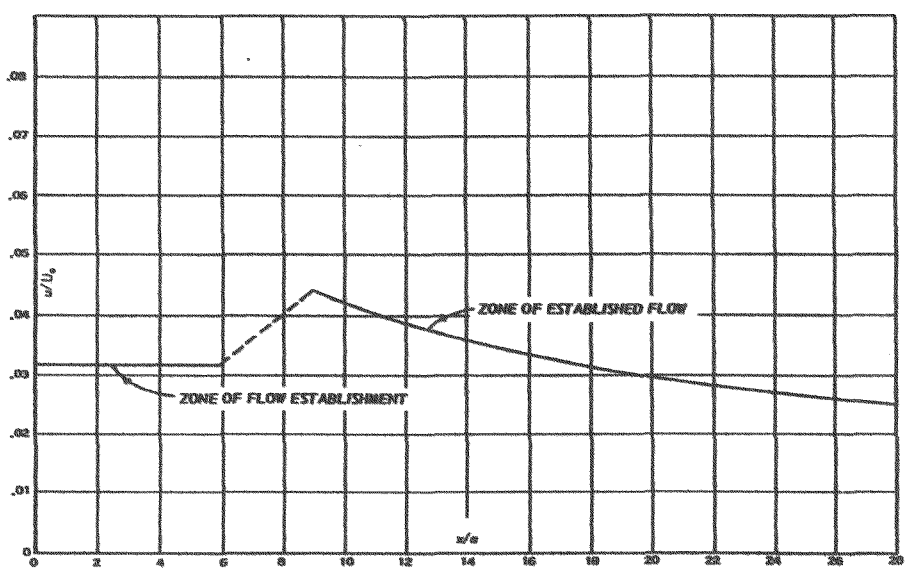

Fig. 19. Velocity of inflow along jet boundary

the curve shown. The interpolated dotted portion of the curve is arbitrary. The actual velocities in this transition zone are unknown, and the straight dotted line in this region has been drawn merely so that the lateral velocity distribution of fig. 19 is consistent with the streamlines $\psi/Q = 0.8$ and above--that is, so that the relation

$$\frac{\psi}{Q} = 0.5 + \frac{1}{Q}\int_0^x v_y\,dx \tag{86}$$

is satisfied.

109. The intersection of the $\psi/Q = 0.7$ streamline with the jet boundary was determined in accordance with the lateral velocity distribution of fig. 19.

110. Inasmuch as the velocity is everywhere tangential to the streamlines, the data of fig. 17 will give the direction of flow at any point. Also, since the velocity at any point in a two-dimensional field of flow is inversely proportional to the spacing of the streamlines, the data of fig. 17 could be used to determine the magnitude of the velocity vector as well as its direction. Nevertheless, it will be more convenient to determine the velocity by other means.

Determination of velocities along streamlines

111. Zone of flow establishment. Tollmien has computed values of $v/U_o \sqrt[3]{2c^2}$ and $u/U_o = F'(\eta)$, and these are shown in table 5. Letting $V = \sqrt{u^2 + v^2}$ we have

$$\frac{V}{U_o} = \left[\left(\sqrt[3]{2c^2}\right)^2 \left(\frac{v}{U_o \sqrt[3]{2c^2}}\right)^2 + \frac{u^2}{U_o^2}\right]^{1/2} \tag{87}$$

112. The ratio of the magnitude of the velocity vector V to the velocity U_o through the slot has been computed from equation 87 and table 5 for various values of η, and the results have been plotted in fig. 20 for the coordinate system of fig. 13.

113. From the data of figs. 17 and 20 the velocity at any point on one of the streamlines may be obtained simply by determining x/a and y/a for the point in question from fig. 17 and using fig. 20 to determine the corresponding velocity ratio V/U_o at that point. Data computed in this

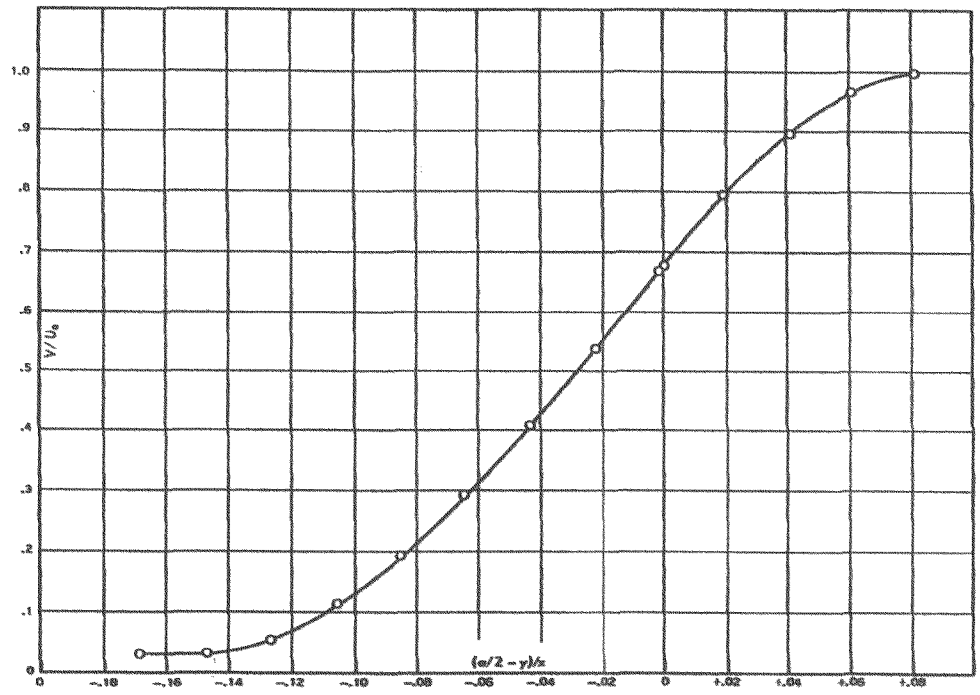

Fig. 20. Velocity distribution in the zone of flow establishment

manner have been plotted against s/a in fig. 21, where s is the distance along the streamline, measured either from the face of the slot or from the jet boundary, whichever is appropriate. In the case of ψ/Q greater than or

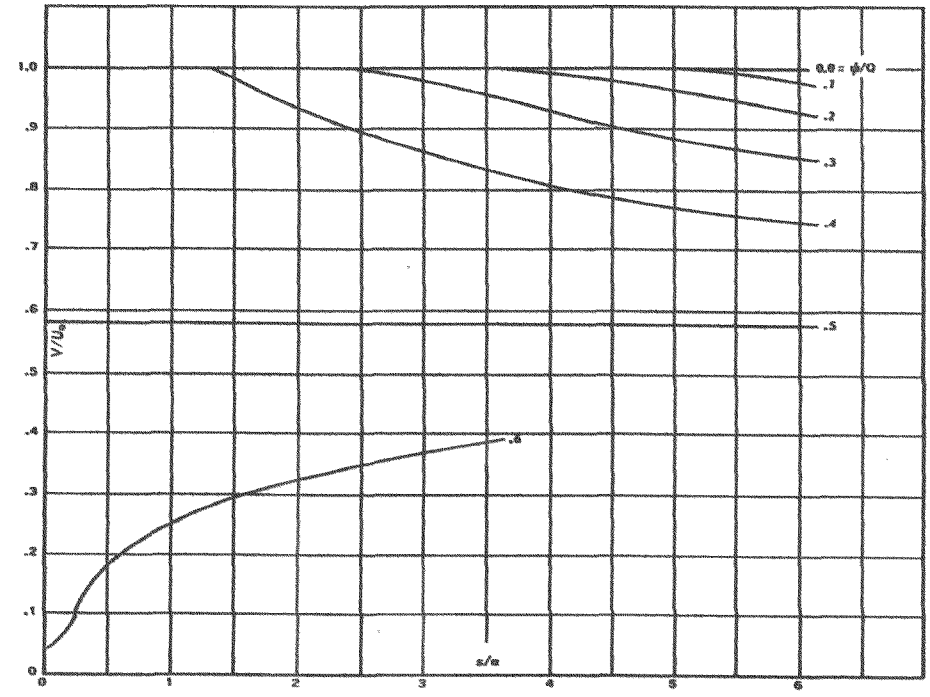

Fig. 21. Velocity along streamlines, zone of establishment

equal to 0.5, s was thus measured from the face of the slot. For ψ/Q greater than 0.5 the initial point was the intersection of the streamline with the jet boundary.

114. Zone of established flow. Eliminating I from equations 79 and 80:

$$U_o^2 x_o = U_{max}^2 x \tag{88}$$

Substituting the value of U_{max} thus obtained into equation 78,

$$\frac{u}{U_o} \sqrt{x/x_o} = F'(\eta) \tag{89}$$

and the function $F'(\eta)$ has been computed by Tollmien and is given in table 5. In like manner the term $\frac{v}{U_o} \sqrt{x/x_o} \frac{1}{\sqrt[3]{2c^2}}$ has been computed by Tollmien. Letting

$$V = \sqrt{u^2 + v^2} \tag{90}$$

we have

$$\frac{V}{U_o} \sqrt{x/x_o} = \left[\left(\frac{u}{U_o} \sqrt{x/x_o} \right)^2 + \left(\frac{v}{U_o} \sqrt{x/x_o} \right)^2 \right]^{1/2} \tag{91}$$

Letting $\sqrt[3]{2c^2} = 0.0989$ as determined previously, the velocity distribution of fig. 22 has been computed from equation 91 and table 5. From the data of figs. 17 and 22, the velocities along the streamlines have been plotted against s/a in fig. 23, where as before s is the distance along the streamline from its intersection either with the face of the slot or with the nominal jet boundary shown in fig. 17.

115. In fig. 24 the data of figs. 21 and 23 for the velocities along the streamlines in the two zones have been combined to give the velocities for the two-dimensional jet issuing from a slot of width a . The curves of fig. 24, together with the stream flow pattern of fig. 17, are sufficient to determine the direction and magnitude of the velocity at any point within the jet and constitute the solution of the problem under discussion. The application of the solution to a specific case is given in Appendix B.

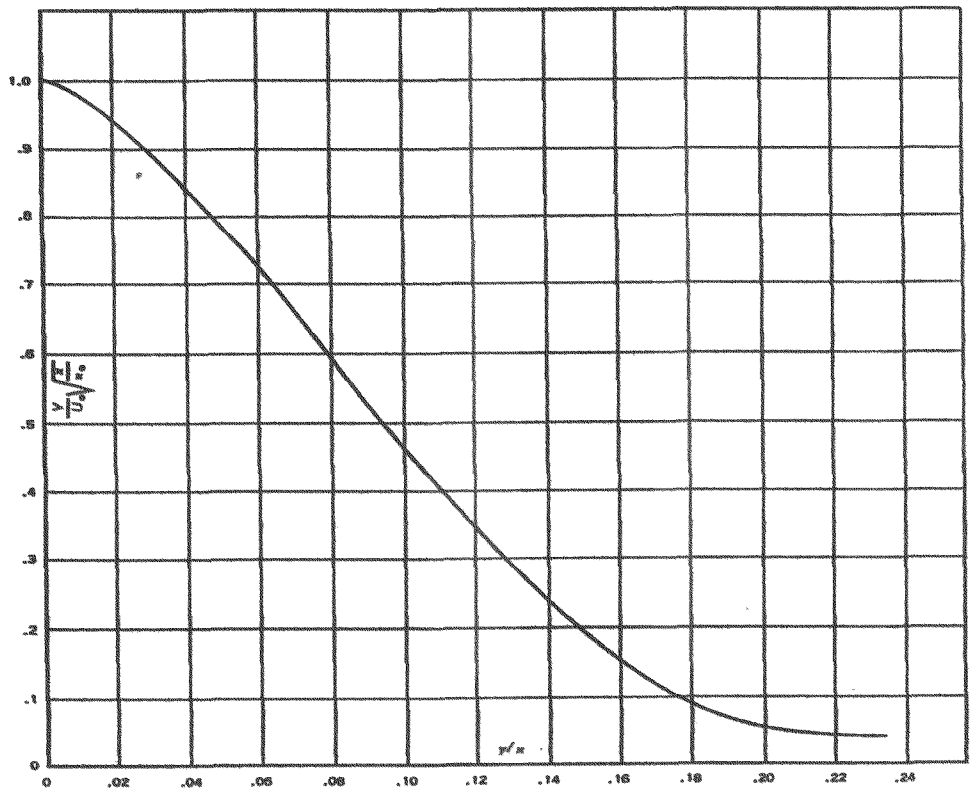

Fig. 22. Velocity distribution in the zone of established flow

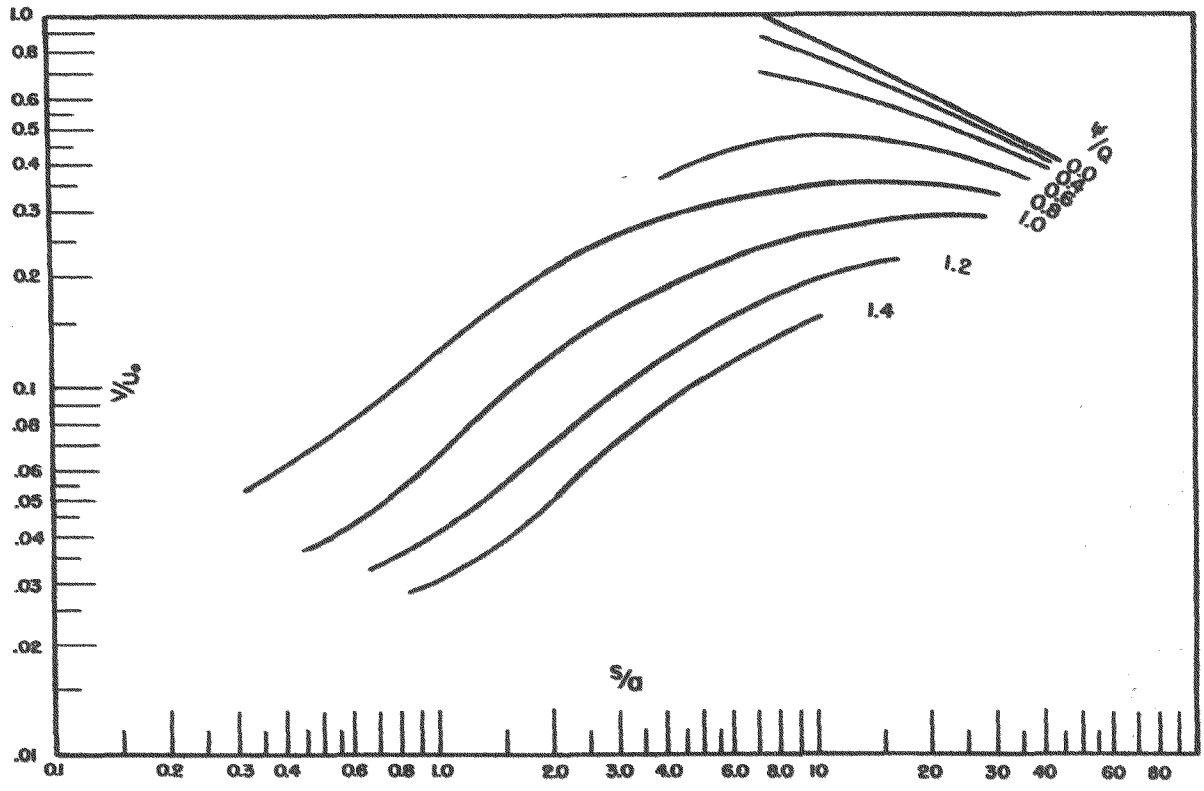

Fig. 23. Velocities along streamlines, zone of established flow

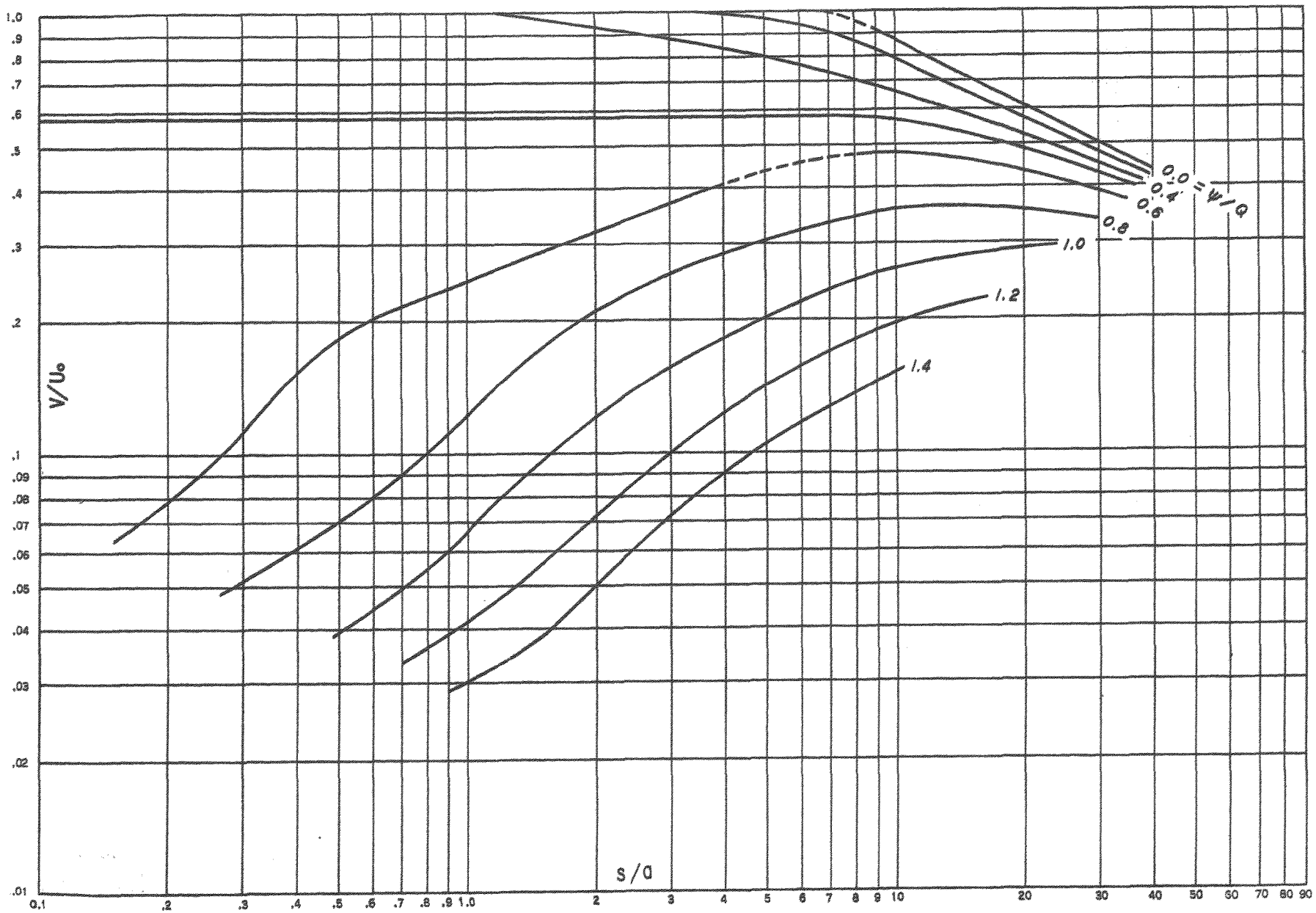

Fig. 24. Velocities along streamlines, two-dimensional jet

Summary

116. On the basis of Tollmien's analysis for the free jet boundary and his analysis of jet flow from a two-dimensional linear slot, the streamlines and the velocities along these streamlines have been determined for a jet issuing from a channel of definite width into an ocean or other large body of water. The solution given assumes at the outset that the flow is essentially two-dimensional. Obviously this will not always be the case in practice. Further, the analysis of Tollmien assumes that Prandtl's mixing length is constant over each lateral section. In the case of an actual ocean and channel this cannot be true, since the mixing length along the bottom of the ocean and at the free surface must be zero.

117. In a channel of more than nominal length connecting a lagoon and ocean, the velocity will not be uniform, as has been assumed herein, but will have the typical horizontal and vertical velocity curves of turbulent channel flow. The action of waves, littoral currents, and density currents, if present, may substantially modify the jet velocity distribution shown. Under these circumstances the solution given must be considered at best as only a first approximation to the velocities actually prevailing. Nevertheless, despite the obvious sources of error mentioned, it is believed that the application of two-dimensional jet theory to the problem of determining the velocity distribution in the stream of water issuing from a channel into an ocean will provide the basic first step for the investigation of the methods of controlling the shoaling in the vicinity of such channel entrances.

Status of Problem

118. Additional research, both experimental and analytical, is warranted on the problem discussed in Part II. In particular the variation of Tollmien's c or the distance x_o with Reynolds number in the region of established flow should be determined by systematic experimentation. In this connection it appears certain that for Reynolds numbers characteristic of the flow prevailing in nature for the problem herein under consideration, turbulence will have developed sufficiently to cause c or x_o

to be independent of the Reynolds number. However, the asymptotic value of c used for this zone has been determined from data obtained at much lower Reynolds numbers and in a region where the data now available indicate that the Reynolds number exerts an appreciable effect. Under these circumstances further experimental investigation of this question would be desirable.

119. Further, it would appear that the conventional jet phenomenon as used herein constitutes only a temporary phase of the flow picture prevailing in the efflux of water from a channel into the tranquil water of an ocean. To be specific, suppose that the connecting channel of fig. 10 were originally absent, and that such a channel were constructed. Initially the flow from the channel would be such as to conform at least approximately, it is believed, to the streamlines shown in fig. 17 and with the velocities along the streamlines shown in fig. 24. However, it is obvious from the streamlines of fig. 17 that deceleration occurs and will cause deposition in the jet area of the suspended or bed load originally eroded from the channel and lagoon.

120. Further, since the water in the jet, as is evident from fig. 17, is being decelerated in the inner core of the jet, while along the boundaries acceleration is occurring, it might be expected that deposition in the region of the boundaries might be at a slower rate than in the inner core of the jet, despite the fact that the acceleration of the water in the region of the jet boundaries is occurring because of the lateral transport of momentum from the inner core with consequent lateral transport of suspended load. In this connection, reference to fig. 6 in Part I indicates, for the reverse of the tidal cycle herein considered--that is, flow from the ocean into the channel--that the acceleration of the water as it approaches the channel entrance is greater in the region of the jet boundaries than in the internal core of the jet. This fact would also indicate the possibility of a marked variation in the net rate of deposition along any lateral section of the jet, with the maximum rate probably occurring in the inner core of the jet.

121. Such deposition of suspended load as envisioned above would, over a period of time, obviously change the streamlines substantially from those shown in fig. 17, and the factor controlling such changes would

be the pattern of deposition of suspended load.

122. It is believed that an investigation of the variation in the net rate of deposition of suspended load implied by the velocity distributions given in Parts I and II herein would be a logical next step in the development of the general problem of shoaling near tidal channels or entrances.

References

1. Albertson, M. L., Dai, Y. B., Jensen, R. A., and Rouse, Hunter, "Diffusion of submerged jets." Trans., American Society of Civil Engineers, vol 115 (1950).
2. Cordes, G., "Untersuchung zur statischen Druckmessung in turbulenter Strömung." Ingenieur-Archiv, vol 8, No. 4 (August 1937), pp 245-270.
3. Forthmann, E., Turbulent Jet Expansion. Technical Memorandum No. 789, National Advisory Committee for Aeronautics, 1936.
4. Goldstein, S., Modern Developments in Fluid Mechanics. Fluid Motion Panel of the Aeronautical Research Committee, Oxford, 1938.
5. Hinze, J. O., and Van Der Hegge Zijnen, B. G., "Transfer of heat and matter in the turbulent mixing zone of an axially symmetrical jet." Applied Scientific Research, vol A1, Nos. 5 through 6 (1949), pp 435-461.
6. Howarth, L., "Concerning the velocity and temperature distribution in plain and axially symmetrical jets." Proc., Cambridge Philosophical Society, vol 34 (1938), p 185.
7. Liepman, Hans Wolfgang, and Laufer, John, Investigations of Free Turbulence. Technical Note No. 1257, National Advisory Committee for Aeronautics, 1947.
8. Okayo, T., and Hasegawa, M., "On the velocity distribution in a plane jet." Proc., Physico-Mathematical Society of Japan, vol 22 (1940).
9. Reichardt, Hans, "Gesetzmässigkeiten der freien Turbulenz." VDI-Forschungsheft, 414 (1942).
10. Tollmien, Walter, "Berechnung turbulenter Ausbreitungs-vorgänge." Zeitschrift für angewandte Mathematik und Mechanik, vol 6 (1926), pp 1-12.
11. Tomotika, S., "Application of the modified vorticity transport theory to the turbulent spreading of a jet of air." Proc., Royal Society of London, vol 165, Series A (March-April 1938).

Table 1

Computed Values of x/b and y/b for Various Values of ψ/Q and $\pi\phi/Q$

Two-Dimensional Orifice

$\frac{\psi}{Q}$	$\frac{\pi\phi}{Q}$	$\frac{x}{b}$	$\frac{y}{b}$
0	-3	1.03	0
	-2	0.605	0
	-1	0.113	0
	-1/2	-0.195	0
	-1/4	-0.380	0
	0	-0.598	0
	1/4	-0.855	0
	1/2	-1.17	0
	3/4	-1.56	0
	1	-2.04	0
	1-1/2	-3.42	
	2	-5.74	0
1/16	0	-0.574	-0.185
	1/4	-0.835	-0.221
	1/2	-1.15	-0.272
	3/4	-1.52	-0.338
	1	-2.01	-0.426
	1-1/2	-3.38	-0.685
	2	-5.64	-1.13
1/8	-3	1.03	-0.157
	-2	0.611	-0.176
	-1	0.129	-0.218
	-1/2	-0.172	-0.266
	-1/4	-0.344	-0.318
	0	-0.538	-0.363
	1/4	-0.784	-0.433
	1/2	-1.07	-0.531
	3/4	-1.44	-0.662
1/8	1	-1.88	-0.831
	1-1/2	-3.18	-1.35
	2	-5.28	-2.20
3/16	0	-0.484	-0.528
	1/4	-0.715	-0.638
	1/2	-0.970	-0.780
	3/4	-1.29	-0.955
	1	-1.70	-1.21
	1-1/2	-2.86	-1.96
	2	-4.76	-3.21
1/4	-3	1.04	-0.319
	-2	0.626	-0.345
	-1	0.159	-0.419
	-1/2	0.0916	-0.508
	-1/4	-0.241	-0.577
	0	-0.404	-0.675
	1/4	-0.595	-0.805
	1/2	-0.821	-0.986
	3/4	-1.09	-1.22
	1	-1.44	-1.54
	1-1/2	-2.44	-2.51
	2	-4.04	-4.07
5/16	0	-0.306	-0.805
	1/4	-0.464	-0.955
	1/2	0.646	-1.16
	3/4	-0.863	-1.44
	1	-1.13	-1.81
	1-1/2	-1.92	-2.94
	2	-3.18	-4.80
3/8	-3	1.06	-0.469
	-2	0.668	-0.509
	-1	0.223	-0.599
	-1/2	-0.0118	-0.704
	-1/4	-0.095	-0.785
	0	-0.203	-0.896
	1/4	-0.315	-1.06
	1/2	-0.455	-1.28
	1	-0.780	-2.01
	1-1/2	-1.31	-3.26
	2	-2.19	-5.32
7/16	0	-0.102	-0.969
	1/4	-0.159	-1.14
	1/2	-0.224	-1.38
	3/4	-0.310	-1.70
	1	-0.395	-2.15
	1-1/2	-0.672	-3.46
	2	-1.12	-5.65
1/2	-3	1.05	-0.627
	-2	0.665	-0.661
	-1	0.284	-0.755
	-1/2	0.102	-0.849
	-1/4	0.041	-0.915
	0	0	0
	1/4	0	-1.16
	1/2	0	-1.40
	3/4	0	-1.74
	1	0	-2.18
	1-1/2	0	-3.52
	2	0	-5.79

Table 2

Computed Values of s/b and q/V for Various Values of ψ/Q and $\pi\phi/Q$

Two-Dimensional Orifice

$\frac{\psi}{Q}$	$\frac{\pi\phi}{Q}$	$\frac{s}{b}$	$\frac{q}{V}$	$\frac{\psi}{Q}$	$\frac{\pi\phi}{Q}$	$\frac{s}{b}$	$\frac{q}{V}$	$\frac{\psi}{Q}$	$\frac{\pi\phi}{Q}$	$\frac{s}{b}$	$\frac{q}{V}$
0	-3	-1.63	0.955	1/4	-3	-1.50	0.966	1/2	-3	-1.19	1.0
	-2	-1.20	0.875		-2	-1.09	0.909		-2	-0.80	1.0
	-1	-0.71	0.695		-1	-0.61	0.775		-1	-0.41	1.0
	-1/2	-0.40	0.560		-1/2	-0.34	0.641		-1/2	-0.19	1.0
	-1/4	-0.22	0.489		-1/4	-0.18	0.559		-3/8	-0.14	1.0
	0	0	0.414		0	0	0.459		-1/4	-0.09	1.0
	1/4	0.26	0.342		1/4	0.23	0.378		0	0	1.0
	1/2	0.58	0.279		1/2	0.53	0.295		1/8	0.08	0.597
	3/4	0.96	0.224		3/4	0.88	0.235		1/4	0.16	0.478
	1	1.44	0.179		1	1.36	0.183		3/8	0.28	0.394
	1-1/2	2.83	0.110		1-1/2	2.73	0.111		1/2	0.40	0.337
	2	5.17	0.0672		2	4.98	0.0694		3/4	0.74	0.251
1/8	-3	-1.57	0.957	3/8	-3	-1.35	0.976		1	1.18	0.191
	-2	-1.16	0.881		-2	-0.95	0.946		1-1/2	2.52	0.113
	-1	-0.67	0.711		-1	-0.51	0.855		2	4.76	0.0679
	-1/2	-0.38	0.582		-1/2	-0.28	0.763				
	-1/4	-0.20	0.504		-1/4	-0.16	0.675				
	0	0	0.426		0	0	0.559				
	1/4	0.26	0.352		1/4	0.20	0.427				
	1/2	0.58	0.282		1/2	0.48	0.322				
	3/4	0.96	0.227		3/4	0.82	0.245				
	1	1.44	0.179		1	1.27	0.188				
	1-1/2	2.44	0.111		1-1/2	2.52	0.112				
	2	4.71	0.0672		2	4.76	0.0675				

Table 3

Computed Values of x/b and y/b for Various Values of ψ/Q and $\pi\phi/Q$ for a Projecting Entrance

$\frac{\psi}{Q}$	$\frac{\pi\phi}{Q}$	$\frac{x}{b}$	$\frac{y}{b}$
0	-5	-1.26	0
	-2	-0.452	0
	-1	0.282	0
	-1/2	0.683	0
	-1/4	0.972	0
	0	1.36	0
	1/4	1.93	0
	1/2	2.76	0
	3/4	4.03	0
	1	6.04	0
	1-1/4	9.23	0
	1-1/2	14.45	0
1/16	0	1.32	0.355
	1/4	1.87	0.516
	1/2	2.64	0.786
	3/4	3.84	1.22
	1	5.64	1.93
	1-1/4	8.64	3.10
	1-1/2	13.55	5.01
1/8	-5	-1.26	0.129
	-2	-0.235	0.172
	-1	0.249	0.250
	-1/2	0.602	0.377
	-1/4	0.852	0.492
	0	1.17	0.670
	1/4	1.62	0.978
	1/2	2.22	1.46
	3/4	3.20	2.26
	1	4.68	3.58
	1-1/4	6.96	5.72
1/8	1-1/2	10.67	9.28
3/16	0	0.960	0.935
	1/4	1.27	1.32
	1/2	1.70	1.98
	3/4	2.25	3.02
	1	3.12	4.72
	1-1/4	4.46	7.54
	1-1/2	6.53	12.19
1/4	-5	-1.27	0.25
	-2	-0.257	0.318
	-1	0.162	0.462
	-1/2	0.416	0.656
	-1/4	0.558	0.832
	0	0.705	1.09
	1/4	0.860	1.53
	1/2	1.02	2.23
	3/4	1.18	3.34
	1	1.34	5.20
	1-1/4	1.49	8.23
	1-1/2	1.65	13.5
5/16	0	0.450	1.17
	1/4	0.450	1.56
	1/2	0.352	2.22
	3/4	0.082	3.24
	1	-0.54	5.01
	1-1/4	-1.58	7.84
	1-1/2	-3.20	12.28
3/8	-5	-1.27	0.377
	-2	-0.29	0.456
3/8	-1	0.054	0.619
	-1/2	0.188	0.784
	-1/4	0.240	0.950
	0	0.226	1.16
	1/4	0.096	1.42
	1/2	-0.216	1.98
	3/4	-0.859	2.76
	1	-1.99	4.07
	1-1/4	-3.98	6.22
	1-1/2	-7.38	9.78
7/16	0	0.068	1.09
	1/4	-0.14	1.26
	1/2	-0.583	1.53
	3/4	-1.48	1.96
	1	-3.03	2.68
	1-1/4	-5.65	3.85
	1-1/2	-10.21	5.77
1/2	-5	-1.27	0.502
	-3	-0.638	0.532
	-2	-0.324	0.586
	-1	-0.043	0.728
	-1/2	0.042	0.861
	-1/4	0.046	0.938
	0	0	1.0
	1/4	-0.22	1.0
	1/2	-0.73	1.0
	3/4	-1.68	1.0
	1	-3.38	1.0
	1-1/4	-6.25	1.0
	1-1/2	-11.15	1.0

Table 4

Computed Values of s/b and q/V for Various Values of ψ/Q and $\pi\phi/Q$

$\frac{\psi}{Q}$	$\frac{\pi\phi}{Q}$	$\frac{s}{b}$	$\frac{q}{V}$
1/2	0	0	1.0
	1/4	0.21	0.229
	1/2	0.73	0.114
	3/4	1.68	0.063
	1	3.37	0.036
	1-1/4	6.25	0.021
3/8	-5	-1.98	0.995
	-2	-0.98	0.879
	-1	-0.60	0.741
	-1/2	-0.38	0.582
	-1/4	-0.21	0.458
	0	0	0.310
	1/4	0.30	0.183
	1/2	0.91	0.104
	3/4	1.94	0.060
	1	3.65	0.036
	1-1/4	6.60	0.021
	1-1/2	11.52	0.013
1/4	-5	-2.30	0.999
	-2	-1.30	0.827
	-1	-0.84	0.599
	-1/2	-0.53	0.405
	-1/4	-0.30	0.308
	0	0	0.217
	1/4	0.49	0.142
	1/2	1.22	0.089
	3/4	3.35	0.056
1/4	1	5.22	0.034
	1-1/4	8.27	0.020
1/8	-5	-2.54	0.987
	-2	-1.53	0.779
	-1	-1.03	0.510
	-1/2	-0.67	0.338
	-1/4	-0.37	0.254
	0	0	0.182
	1/4	0.56	0.124
	1/2	1.32	0.082
	3/4	2.77	0.052
	1	4.77	0.032
	1-1/4	7.87	0.020
0	-5	-2.60	0.986
	-2	-1.58	0.765
	-1	-1.08	0.487
	-1/2	-0.66	0.319
	-1/4	-0.38	0.239
	0	0	0.172
	1/4	0.56	0.118
	1/2	1.40	0.078
	3/4	2.78	0.050
	1	4.78	0.0317
	1-1/4	7.87	0.0197

Table 5

Tollmien's Computed Data for Two-Dimensional Jet Flow

Free Jet Boundary				Jet From Linear Slot			
$= \frac{y}{x\sqrt[3]{2c^2}}$	$F'(\eta) = \frac{u}{U_o}$	$F(\eta) = \frac{\psi}{U_o x \sqrt[3]{2c^2}}$	$\frac{v}{U_o\sqrt[3]{2c^2}}$	η	$F'(\eta) = \frac{u}{U_{max}}$	$F(\eta) = \frac{\psi}{U_o\sqrt{x_o}\sqrt{x}\sqrt[3]{2c^2}}$	$\frac{v\sqrt{x}}{U_o\sqrt{x_o}\sqrt[3]{2c^2}}$
0.981	1.0	0.981	0.0	0.0	1.0	0.0	0.0
0.731	0.969	0.732	-0.022	0.05	0.995	0.050	0.025
0.481	0.895	0.500	-0.069	0.10	0.979	0.099	0.049
0.231	0.791	0.286	-0.104	0.15	0.962	0.148	0.070
-0.019	0.668	0.104	-0.117	0.20	0.940	0.195	0.091
-0.269	0.538	-0.047	-0.096	0.40	0.842	0.374	0.150
-0.519	0.411	-0.166	-0.047	0.60	0.721	0.530	0.168
-0.769	0.296	-0.254	0.027	0.80	0.604	0.664	0.151
-1.019	0.193	-0.312	0.115	1.0	0.474	0.766	0.091
-1.269	0.112	-0.351	0.209	1.2	0.357	0.850	0.003
-1.519	0.049	-0.371	0.297	1.4	0.254	0.910	-0.099
-1.769	0.012	-0.379	0.358	1.6	0.165	0.951	-0.212
-2.019	0.0	-0.379	0.379	1.8	0.095	0.976	-0.318
				2.0	0.046	0.989	-0.402
				2.2	0.013	0.995	-0.469
				2.4	0.000	0.996	-0.498

APPENDIX A: APPLICATION OF A CONTRACTING FLOW NET TO A SPECIFIC CONDITION

1. Part I of the main report gives a general solution to the problem of direction and velocity of flow entering a confined channel. This appendix applies the general solution to a specific case. The case selected assumes the following:

Width of channel, 1000 ft

Average flow velocity in channel, 2.0 ft per sec

Depth of channel, not pertinent. Depth over entire flow area assumed uniform

2. The flow net is drawn up using table 2 and fig. 5 of the main report as described in the following paragraphs.

3. First, compute the free streamline velocity, V , from the formula (see page 11 of main report):

$$V = V_m/0.611$$

where V_m is the mean velocity in the channel. V in this case is the velocity of the free streamline after it enters the channel; it is also the velocity of all streamlines at an infinite distance downstream from the entrance assuming nonviscous flow. In the case at hand:

$$V = V_m/0.611 = 2.0/0.611$$

$$V = 3.27 \text{ ft per sec}$$

4. Next enter table 2 and convert the q/V column into q by multiplying the q/V value by 3.27. The symbol q represents the velocity at the indicated location. (This conversion is made in table A1 of this appendix.)

5. Using fig. 5, plot those computed values of q at the proper intersection of the ψ/Q and $\pi\phi/Q$ coordinates as shown in fig. 5.

6. Convert the x and y grid in fig. 5 to a dimensioned grid by multiplying the nondimensional x and y coordinates as shown in fig. 5 by one-half the channel width (in this case by one-half of 1000 or 500 ft). The results of this conversion are shown in fig. A1 of this appendix.

7. The resulting diagram is a plot of the flow velocity and direction at the selected points in the flow net for the assumed conditions. It is of interest to note that the maximum velocities at the entrance are

found near the outer boundaries of the channel rather than in the center of the channel in this type of solution.

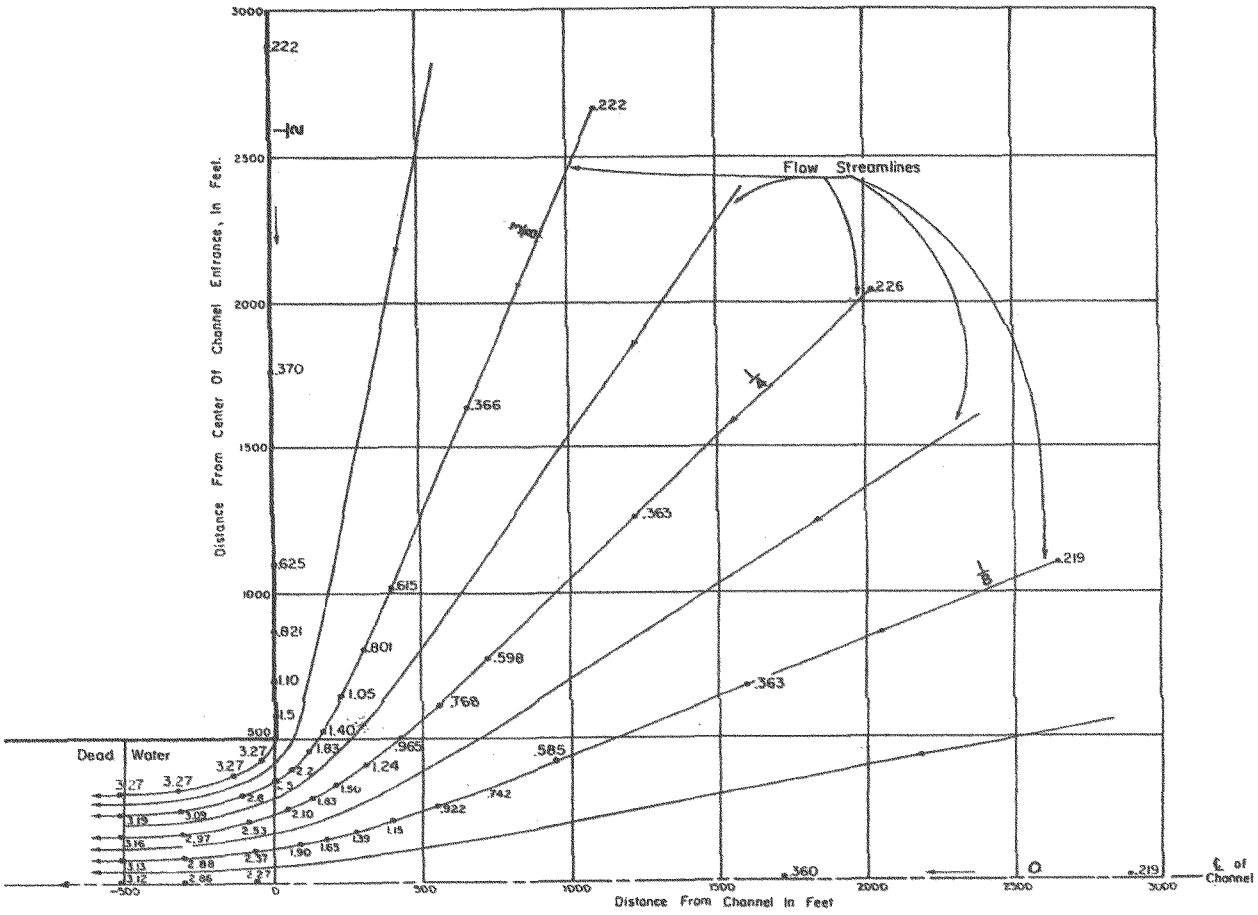

Fig. A1. Example of velocity distribution at entrance to a two-dimensional channel. Assumed width of channel is 1000 ft and assumed mean velocity through channel is 2.0 ft/sec. (Note: Only one-half of channel and flow pattern is shown.)

Table A1

Calculations for Velocity Over a Converging Flow Net

$$q = 3.27\left(\frac{q}{V}\right)$$

$\frac{\psi}{Q}$	$\frac{\pi\phi}{Q}$	$\frac{q}{V}$	q
0	-3	0.955	3.12
	-2	0.875	2.86
	-1	0.695	2.27
	-1/2	0.560	1.83
	-1/4	0.489	1.60
	0	0.414	1.35
	1/4	0.342	1.12
	1/2	0.279	0.912
	3/4	0.224	0.732
	1	0.179	0.585
	1-1/2	0.110	0.360
	2	0.0672	0.219
1/8	-3	0.957	3.13
	-2	0.881	2.88
	-1	0.711	2.32
	-1/2	0.582	1.90
	-1/4	0.504	1.65
	0	0.426	1.39
	1/4	0.352	1.15
	1/2	0.282	0.922
	3/4	0.227	0.742
	1	0.179	0.585
	1-1/2	0.111	0.363
	2	0.0672	0.219

$\frac{\psi}{Q}$	$\frac{\pi\phi}{Q}$	$\frac{q}{V}$	q
1/4	-3	0.966	3.16
	-2	0.909	2.97
	-1	0.775	2.53
	-1/2	0.641	2.10
	-1/4	0.559	1.83
	0	0.459	1.50
	1/4	0.378	1.24
	1/2	0.295	0.965
	3/4	0.235	0.768
	1	0.183	0.598
	1-1/2	0.111	0.363
	2	0.0694	0.226
3/8	-3	0.976	3.19
	-2	0.946	3.09
	-1	0.855	2.80
	-1/2	0.763	2.50
	-1/4	0.675	2.21
	0	0.559	1.83
	1/4	0.427	1.40
	1/2	0.322	1.05
	3/4	0.245	0.801
	1	0.188	0.615
	1-1/2	0.112	0.366
	2	0.0675	0.222

$\frac{\psi}{Q}$	$\frac{\pi\phi}{Q}$	$\frac{q}{V}$	q
1/2	-3	1.0	3.27
	-2	1.0	3.27
	-1	1.0	3.27
	-1/2	1.0	3.27
	-3/8	1.0	3.27
	-1/4	1.0	3.27
	0	1.0	3.27
	1/8	0.597	1.95
	1/4	0.478	1.56
	3/8	0.394	1.29
	1/2	0.337	1.10
	3/4	0.251	0.821
	1	0.191	0.625
	1-1/2	0.113	0.370
	2	0.679	0.222

APPENDIX B: APPLICATION OF AN EXPANDING FLOW NET TO A SPECIFIC CONDITION

1. Part II of the main report gives a general solution to the problem of direction and velocity of flow leaving a confined channel. The problem is essentially that of a two-dimensional jet. This appendix applies the general solution to a specific case. The case assumes the following:

Width of jet at exit, 500 ft

Average flow velocity in channel before exit, 3.0 ft per sec

Depth of channel, not pertinent. Depth over entire area of flow assumed uniform

2. The flow net is drawn by first referring to fig. 17 of the main report. The coordinates in fig. 17 are converted to dimensioned quantities by multiplying the x/a and y/a coordinates by 500 ft, the assumed width of the jet at exit. This is done to construct the coordinate background of fig. B1.

3. The velocities to be computed will fall on the ψ/Q streamlines shown in fig. 17. This required the measurement of a value, s/a, from fig. 17; s/a is the distance measured along these streamline curves using the dashed line as the zero point for all streamlines greater than 0.5, and the exit point of the jet for the 0.5 and all lesser streamlines. This distance is measured and its value is determined by its equivalent length on the x/a coordinate scale. Table B1 shows the compilation of the s/a value for four of the ψ/Q streamlines (1.4, 1.2, 1.0, and 0.2).

4. Fig. 23, which shows a diagram of V/U_o as a function of s/a values along the streamlines, ψ/Q, is then utilized (V = velocity at selected point and U_o = exit velocity of jet). For each s/a value on the selected ψ/Q streamline the value of V/U_o is read from the diagram of fig. 23. The velocity is then determined by multiplying the V/U_o value by 3.0 ft per sec, the assumed exit velocity of the jet. This process is repeated for a sufficient number of the ψ/Q streamlines to give the desired definition of the flow pattern. The results of these steps for four selected streamlines are shown in the fourth, fifth, and sixth columns of table B1.

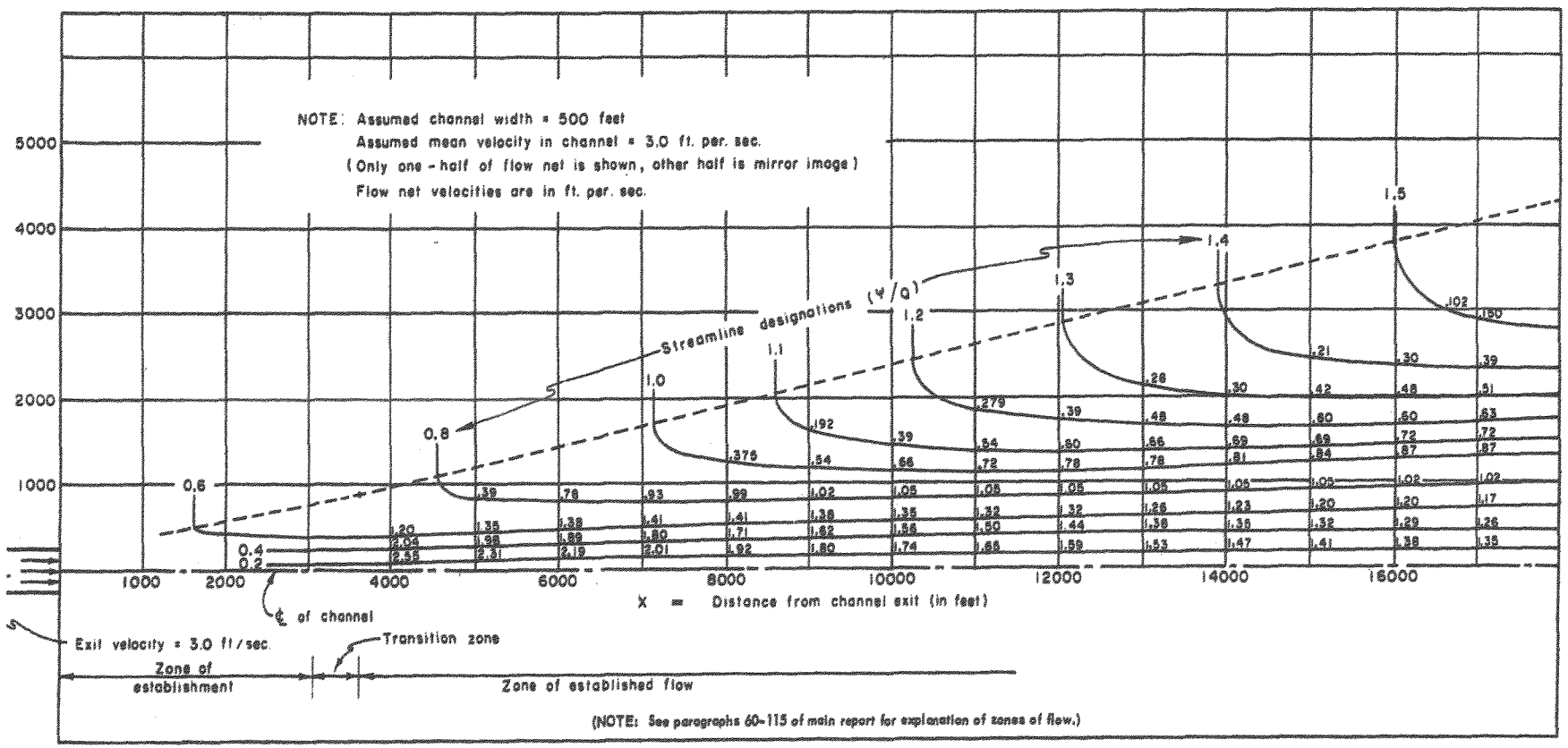

Fig. B1. Example of velocity distribution at exit from a two-dimensional channel

5. These steps were followed in constructing the velocity flow net shown in fig. B1. The applicable values of the x and y coordinates of fig. B1 are shown in table B1, and are obtained by multiplying the x/a and y/a values in the table by 500 ft, the assumed exit width of the jet.

6. The zones of flow which are indicated in fig. B1 are explained in paragraphs 60 through 115 of the report. In effect, these zones define the transition of the flow from a streamlined, unidirectional jet to a dispersive, turbulent flow expanding into the larger body of water. The zone labeled "transition zone" in fig. B1 is not specifically defined in the text; however, it represents the sector between the end of the "zone of establishment" at x/a = 6.12 and the beginning of the "zone of established flow" at x/a = 7.27.

Table B1

Calculations of Velocity Over a Diverging Flow Net

$\frac{\psi}{Q}$	$\frac{x}{a}$	$\frac{y}{a}$	$\frac{s}{a}$	$\frac{V}{U_o}$	V	x	y
1.4	36	4.6	8.7	0.14	0.42	18,000	2300
1.4	34	4.7	6.7	0.13	0.39	17,000	2350
1.4	32	4.8	4.7	0.10	0.30	16,000	2400
1.4	30	4.9	2.9	0.070	0.21	15,000	2450
1.4	28	6.1	0.5			14,000	3050
1.4	27.8	6.6	0			13,900	3300
1.2	36	3.5	16.1	0.22	0.66	18,000	1750
1.2	34	3.5	14.1	0.21	0.63	17,000	1750
1.2	32	3.4	12.1	0.20	0.60	16,000	1700
1.2	30	3.3	10.1	0.20	0.60	15,000	1650
1.2	28	3.3	8.1	0.16	0.48	14,000	1650
1.2	26	3.4	6.1	0.16	0.48	13,000	1700
1.2	24	3.5	4.1	0.13	0.39	12,000	1750
1.2	22	3.7	2.1	0.093	0.279	11,000	1850
1.2	20.5	4.8	0			10,250	2400
1.0	36	2.7	22.1	0.29	0.87	18,000	1350
1.0	34	2.6	20.1	0.29	0.87	17,000	1300
1.0	32	2.5	18.1	0.29	0.87	16,000	1250
1.0	30	2.5	16.1	0.28	0.84	15,000	1250
1.0	28	2.4	14.1	0.27	0.81	14,000	1200
1.0	26	2.3	12.1	0.26	0.78	13,000	1150
1.0	24	2.3	10.1	0.26	0.78	12,000	1150
1.0	22	2.4	8.1	0.24	0.72	11,000	1200
1.0	20	2.4	6.1	0.22	0.66	10,000	1200
1.0	18	2.4	4.1	0.18	0.54	9,000	1200
1.0	16	2.5	2.1	0.125	0.375	8,000	1250
1.0	14.3	3.4	0			7,150	1700
0.2	32	0.4	32	0.46	1.38	16,000	200
0.2	28	0.4	28	0.49	1.47	14,000	200
0.2	24	0.3	24	0.53	1.59	12,000	150
0.2	20	0.3	20	0.58	1.74	10,000	150
0.2	16	0.3	16	0.64	1.92	8,000	150
0.2	12	0.3	12	0.73	2.19	6,000	150
0.2	8	0.2	8	0.85	2.55	4,000	100